T · H · E
OHIO
STATE
UNIVERSITY

MICROWAVE ANTENNA TECHNOLOGY

CALCULATION OF FIELDS RADIATED BY ROTATIONALLY SYMMETRIC HORN ANTENNAS USING MOMENT METHOD

by

C.W. Chuang

T.H. Lee

The Ohio State University

ElectroScience Laboratory

Department of Electrical Engineering
Columbus, Ohio 43212

Technical Report 717822-6

NOTICES

When Government drawings, specifications, or other data are used for any purpose other than in connection with a definitely related Government procurement operation, the United States Government thereby incurs no responsibility nor any obligation whatsoever, and the fact that the Government may have formulated, furnished, or in any way supplied the said drawings, specifications, or other data, is not to be regarded by implication or otherwise as in any manner licensing the holder or any other person or corporation, or conveying any rights or permission to manufacture, use, or sell any patented invention that may in any way be related thereto.

F6383 #4

50272-101

REPORT DOCUMENTATION PAGE	1. REPORT NO.	2.	3. Recipient's Accession No.

4. Title and Subtitle
MICROWAVE ANTENNA TECHNOLOGY: Calculation of Fields Radiated by Rotationally Symmetric Horn Antennas Using Moment Method

5. Report Date
May 1987

6.

7. Author(s)
C.W. Chuang and T.H. Lee

8. Performing Organization Rept. No.
717822-6

9. Performing Organization Name and Address
The Ohio State University ElectroScience Laboratory
1320 Kinnear Road
Columbus, Ohio 43212

10. Project/Task/Work Unit No.

1

13. Type of Report & Period Covered
Technical

14.

15. Supplementary Notes

16. Abstract (Limit: 200 words)

The radiation problems of microwave horn antennas which are circularly symmetric (bodies of revolution) can be analyzed by the method of moments. With this approach, the induced currents on the horn surface can be decomposed into longitudinal and azimuthal components. Each current component is expanded in series form with piece-wise sinusoidal basis functions and the amplitude of each current sample is solved. From the resulting surface currents, the radiation patterns of the horn are calculated. This report summarizes this method and compares the calculated patterns with measured patterns for several horn antennas, including conical horns, corrugated horns and dual mode horns.

17. Document Analysis a. Descriptors

b. Identifiers/Open-Ended Terms

c. COSATI Field/Group

18. Availability Statement	19. Security Class (This Report)	21. No. of Pages
Approved for public release; distribution is unlimited.	Unclassified	84
	20. Security Class (This Page) Unclassified	22. Price

(See ANSI-Z39.18) See Instructions on Reverse

OPTIONAL FORM 272 (4-77)
(Formerly NTIS-35)
Department of Commerce

TABLE OF CONTENTS

LIST OF FIGURES

I. INTRODUCTION

The problem of electromagnetic radiation and scattering from perfectly conducting bodies of revolution of arbitrary shape has been studied by Mautz and Harrington [1]. An integro-differential equation was obtained from the potential integrals plus boundary conditions at the body and was solved by the method of moments. The simplification derived from a rotationally symmetric body is that all physical quantities can be expanded in Fourier series in the azimuth coordinate and quantities of different harmonics can be treated independently. A slightly different formulation based on the reaction theorem was also used by Chuang [2] to solve the same type of radiation and scattering problem.

In this report, the same formulation given in [2] is employed to set up generalized network equations for perfectly conducting bodies of revolution for application to the radiation problem of conical-type horn antennas. These antennas include smooth-wall conical horns, corrugated horns and dual-mode horns. The corrugated horn pattern is simulated by the H-plane pattern of a conical horn with the same inner dimension as the corrugated horn and is assumed to be circularly symmetric. Several examples are shown and compared with measured patterns in order to validate this approach. Appendix A shows the detailed derivation of the elements associated with the impedance matrix. The Body of Revolution Code has been modified and implemented into the OSU Reflector Antenna Code. One can look at the BR: Command of the User's Manual of the Reflector Antenna Code for more detail.

II. REACTION FORMULATION

Consider a primary source of an electric current $\bar{J}_i$ illuminating a perfectly conducting horn type scatterer. The scatterer occupies a volume T enclosed by a surface S as shown in Figure 2.1(a). Currents are induced on the scatterer which in turn will radiate such that the total fields are

$$\bar{E} = \bar{E}^i + \bar{E}^s \quad ,$$
$$\bar{H} = \bar{H}^i + \bar{H}^s \quad , \tag{1}$$

where $\bar{E}^i$, $\bar{H}^i$ and $\bar{E}^s$, $\bar{H}^s$ are the primary and scattered fields, respectively.

Now let us assume that the horn walls have zero thickness and replace the scatterer with free space as shown in Figure 2.1(b). From the equivalence principle, one can use the equivalent surface current $\vec{J}_s$ to find the total scattered field. The surface current $\vec{J}_s$ on the surface S is given by

$$\vec{J}_s = \hat{n} \times (\vec{H}_1 - \vec{H}_2) \tag{2}$$

while the magnetic surface current $\vec{M}_s$ vanishes since the scatterer is a perfect conductor. In Equation (2), $\hat{n}$ is the unit outward normal to the surface and $\vec{H}_1$ and $\vec{H}_2$ are the total scattered fields outside and inside the horn. Further let us introduce an arbitrary current $\vec{J}_m$ into region

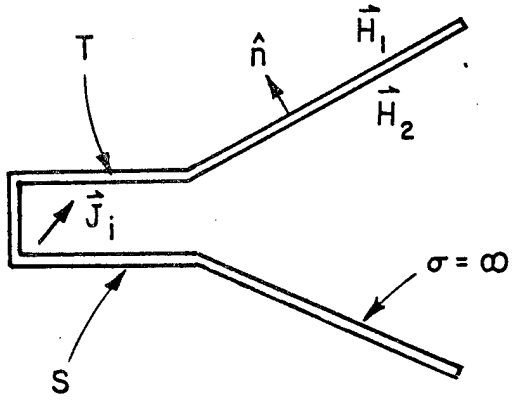

(a) original problem

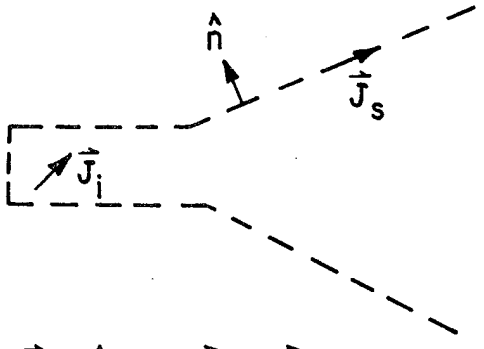

$$\vec{J}_s = \hat{n} \times (\vec{H}_1 - \vec{H}_2)$$

(b) free space equivalence

Figure 2.1. Geometry of horn scattering problem.

T originally occupied by the scatterer. Assume that $\vec{J}_m$ will radiate fields $\vec{E}^m$, $\vec{H}^m$ into free space. Then from the reciprocity theorem we arrive at the reaction equation

$$\int_S \bar{E}^m \cdot \vec{J}_s \, ds = \int_T \bar{E}^s \cdot \vec{J}_m \, d\nu$$

$$= - \int_T \bar{E}^i \cdot \vec{J}_m \, d\nu$$

$$= - \int_{\nu_i} \bar{E}^m \cdot \vec{J}_i \, d\nu \qquad (3)$$

Note that the volume integral is performed over the region T as shown in Figure 2.1(a) although the thickness of the horn surface is assumed zero. The condition $\vec{E} = \vec{E}^i + \vec{E}^s = 0$ on the surface has been used in Equation (3). The last integral in Equation (3) is performed over the region ν_i where the source $\vec{J}_i$ is located.

Let the z-axis be the axis of revolution and t the distance measured along a profile line of the conducting body as shown in Figure 2.2. Because of the orthogonality of Fourier series, different harmonics in azimuth coordinate (ϕ) can be considered separately. For each harmonic, the induced currents on the conducting body can be written as

$$\bar{J}_s = \hat{t} \, f(t) \begin{Bmatrix} \cos m\phi \\ \sin m\phi \end{Bmatrix} + \hat{\phi} g(t) \begin{Bmatrix} \sin m\phi \\ -\cos m\phi \end{Bmatrix} \qquad (4)$$

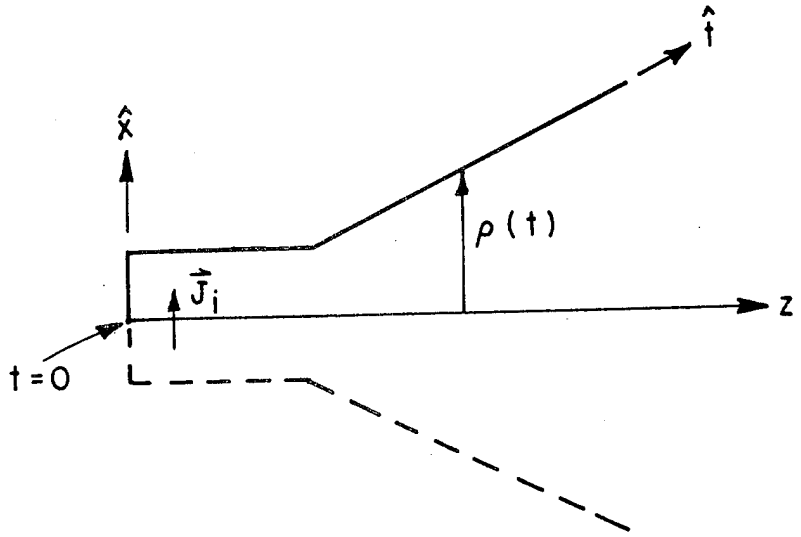

Figure 2.2. Coordinate system for horn scattering calculation by moment method.

where m can be zero or any positive integer. For a conical type horn antenna, we choose a short electric current dipole oriented in the x-direction and located on the z-axis inside the horn as the primary source. Therefore only the upper sinusoidal function in (4) will be used with m=1.

Following standard procedures of moment methods, Equation (4) is then expanded in a finite series

$$\bar{J}_S = \sum_n \hat{t}\, I_n^t \frac{Q_n(t)}{k\rho(t)} \cos m\phi + \hat{\phi} I_n^{\phi} P_n(t) \sin m\phi \qquad (5)$$

where $\rho(t)$ is the distance from a point t on the surface to the axis of revolution as shown in Figure 2.2. $Q_n(t)$ and $P_n(t)$ are expansion functions defined as

$$Q_n(t) = \frac{\sin k(t-t_{n-1})}{\sin k(t_n-t_{n-1})}, \qquad \text{if } t_n \geq t \geq t_{n-1}$$

$$= \frac{\sin k(t_{n+1}-t)}{\sin k(t_{n+t}-t_n)}, \qquad \text{if } t_n \leq t \leq t_{n+1}$$

$$= 0 \qquad , \qquad \text{otherwise,} \qquad (6)$$

and

$$P_n(t) = 1 , \qquad \text{if } t_n \leq t \leq t_{n+1}$$

$$= 0 , \qquad \text{otherwise,} \qquad (7)$$

where t_i are sampling points along the generating profile line of the body of revolution as shown in Figure 2.3(a).

If the test sources are chosen to be the same as the expansion currents, Equation (3) then reduces to a matrix equation,

$$\begin{bmatrix} [Z^{tt}] & [Z^{t\phi}] \\ [Z^{\phi t}] & [Z^{\phi\phi}] \end{bmatrix} \begin{bmatrix} [I^t] \\ [I^\phi] \end{bmatrix} = \begin{bmatrix} [V^t] \\ [V^\phi] \end{bmatrix} . \qquad (8)$$

The elements of the various matrices are

$$Z_{ln}^{tt} = -\int \hat{t} \cos m\phi \frac{Q_n(t)}{k\rho(t)} \cdot \bar{E}^{tl} \, ds$$

$$Z_{ln}^{t\phi} = -\int \hat{\phi} \sin m\phi \, P_n(t) \cdot \bar{E}^{tl} \, ds$$

$$Z_{ln}^{\phi t} = -\int \hat{t} \cos m\phi \frac{Q_n(t)}{k\rho(t)} \cdot \bar{E}^{\phi l} \, ds$$

$$Z_{ln}^{\phi\phi} = -\int \hat{\phi} \sin m\phi \, P_n(t) \cdot \bar{E}^{\phi l} \, ds$$

$$V_l^t = \int \hat{t} \cos m\phi \frac{Q_l(t)}{k\rho(t)} \cdot \bar{E}^i \, ds$$

$$V_l^\phi = \int \hat{\phi} \sin m\phi \, P_l(t) \cdot \bar{E}^i \, ds \qquad (9)$$

with m=1.

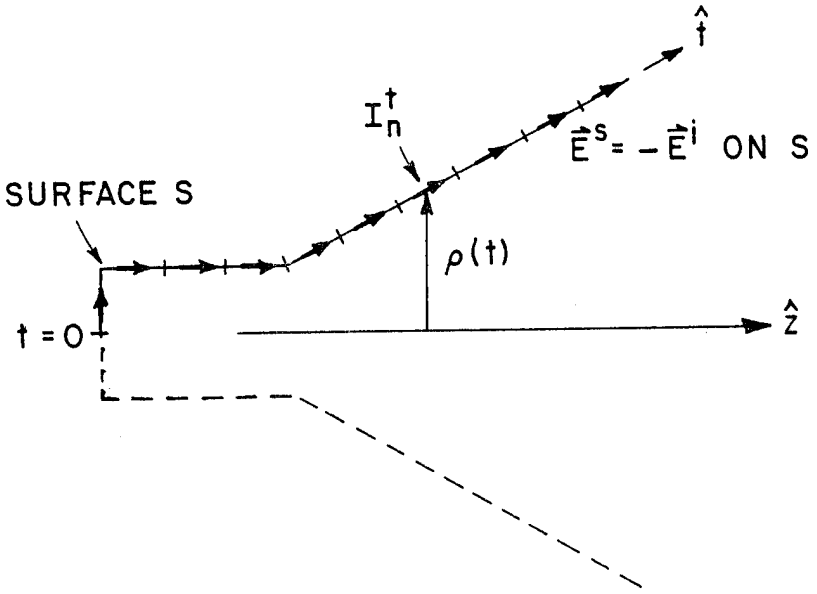

(a) scattered field produced by horn wall currents

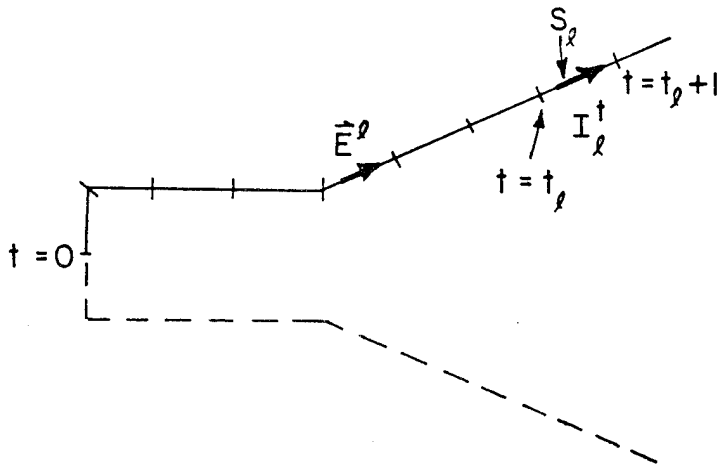

(b) field $\vec{E}^1$ from single expansion current $I_1^t\ \hat{t}$

Figure 2.3. Expansion of the surface current $\vec{J}_s$.

Note that $\bar{E}^{t1}$ and $\bar{E}^{\phi 1}$ are electric fields generated by electric current modes I_1^t and I_1^ϕ, respectively. From the reciprocity theorem it can be shown that the impedance matrix is symmetric.

A. The Impedance Matrix

In this section the impedance elements will be discussed in detail. From Equation (9) the impedance elements have the general form:

$$Z_{ln} = -\int \bar{J}_n \cdot \bar{E}^l \, ds$$

$$= j\omega \int \bar{J}_n \cdot \left[\bar{A}^l + \frac{1}{k^2} \nabla\nabla \cdot \bar{A}^l\right] ds$$

$$= j\omega \int \left[\bar{J}_n \cdot \bar{A}^l - \frac{1}{k^2} \left(\nabla \cdot \vec{J}_n\right)\left(\nabla \cdot \bar{A}^l\right)\right] ds$$

$$= \frac{j\omega\mu_o}{4\pi} \iint \left[\bar{J}_n \cdot \bar{J}_l - \frac{1}{k^2} \left(\nabla \cdot \bar{J}_n\right)\left(\nabla' \cdot \bar{J}_l\right)\right] \frac{e^{-jkR}}{R} \, ds' \, ds \tag{10}$$

The derivation of this equation is given in Appendix A (in detail). In view of the following formulas,

$$\nabla \cdot \bar{J} = \frac{1}{\rho} \frac{\partial}{\partial t} (\rho J_t) + \frac{1}{\rho} \frac{\partial}{\partial \phi} (J_\phi) \, , \tag{11}$$

$$\hat{t}\cdot\hat{t}' = \sin\xi\,\sin\xi'\,\cos(\phi-\phi') + \cos\xi\,\cos\xi' \ ,$$

$$\hat{t}\cdot\hat{\phi}' = \sin\xi\,\sin(\phi-\phi') \ ,$$

$$\hat{\phi}\cdot\hat{t}' = -\sin\xi'\,\sin(\phi-\phi') \ ,$$

$$\hat{\phi}\cdot\hat{\phi}' = \cos(\phi-\phi') \qquad (12)$$

where ξ is the angle between $\hat{t}$ and $\hat{z}$, the various impedance elements become

$$Z_{ln}^{tt} = \frac{j\omega\mu_o}{4k^2}\iint\left\{\left[\sin\xi\,\sin\xi'(G_{m+1}+G_{m-1})+2\,\cos\xi\,\cos\xi' G_m\right]Q_n(t)Q_l(t')\right.$$

$$\left. - \frac{2}{k^2}\,G_m\,Q_n'(t)Q_l'(t')\right\}dt\cdot dt' \ ,$$

$$Z_{ln}^{t\phi} = \frac{j\omega\mu_o}{4k^2}\iint\left\{k\rho\sin\xi'(G_{m+1}-G_{m-1})P_n(t)Q_l(t')-\frac{2m}{k}\,G_m P_n(t)Q_l'(t')\right\}dt\cdot dt' ,$$

$$Z_{ln}^{\phi t} = \frac{j\omega\mu_o}{4k^2}\iint\left\{k\rho'\sin\xi(G_{m+1}-G_{m-1})Q_n(t)P_l(t')-\frac{2m}{k}\,G_m Q_n'(t)P_l(t')\right\}dt\cdot dt' ,$$

$$Z_{ln}^{\phi\phi} = \frac{j\omega\mu_o}{4k^2}\iint\left\{k\rho\rho'(G_{m+1}+G_{m-1}) - 2m^2\,G_m\right\}P_n(t)P_l(t')dt\cdot dt' ,$$

$$Z_{ln}^{\phi t} = Z_{nl}^{t\phi} \ . \qquad (13)$$

These equations are derived in detail in Appendix A.

The variables in Equations (13) are defined as follows:

$$G_m = \int_0^{\pi} \cos m\phi \, \frac{e^{-jkR}}{R} \, d\phi \, , \tag{14}$$

$$R = \left[(z-z')^2 + (\rho-\rho)^2 + 4\rho\rho' \sin^2 \frac{\phi}{2}\right]^{\frac{1}{2}} . \tag{15}$$

The evaluation of G_m has been discussed in detail by Mautz and Harrington [1].

B. Excitation Column

The primary source $\vec{J}_i$ is chosen to be an x-directed on-axis electric dipole with dipole strength P_x. The excitation element V_l^t associated with one of the monopoles of the current $\hat{t}\, J_l^t$ is given by

$$V_l^t = \int_S \hat{t}\, J_l^t \cdot \vec{E}^i \, ds'$$

in which $\vec{E}^i$ is the electric field radiated by the primary source $\vec{J}_i$ and the integration is carried over a ring of surface current. From reciprocity, one can calculate V_l^t by

$$V_l^t = \int_{v_i} \vec{J}_i \cdot \vec{E}_l \, dv$$

where $\vec{E}_1$ is the electric field radiated by the current mode $\hat{t}\, J_1^t$ and the integration is carried over the space at which the primary source is located. Since the primary source is an on-axis dipole, one can express $\vec{J}^i$ as

$$\vec{J}^i = \hat{x}\, P_x \delta(x)\delta(y)\delta(z-z_o)$$

where $\delta(x)\delta(y)\delta(z-z_o)$ indicates the dipole is located at $(0,0,z_o)$. Thus, V_1^t is calculated by the following equation

$$V_1^t = \hat{x}\, P_x \cdot \vec{E}_1(0,0,z_o) \ .$$

The geometry for the calculation of $\vec{E}_1(0,0,z_o)$ is shown in Figure 2.4. The monopole is located between $t=t_1$ and $t=t_2$ with P being the field point. The current distribution on the monopole is given by

$$\hat{t}\, J_1^t = \hat{t}\, \frac{1}{k\rho(t)} \, \frac{I_1 \sin\left[k(t_2-t)\right] + I_2 \sin\left[k(t-t_1)\right]}{\sin kd} \cos m\phi$$

since piece-wise sinusoidal functions have been used to expand the surface current. The electric field $\vec{E}_1(0,0,z_o)$ radiated by $\hat{t}\, J_1^t$ can be found by the following equation

$$\vec{E}_1 = - j\omega\mu_o \vec{A}_1 - \nabla\Phi$$

where $\vec{A}_1$ is the magnetic vector potential and Φ is the scalar potential.

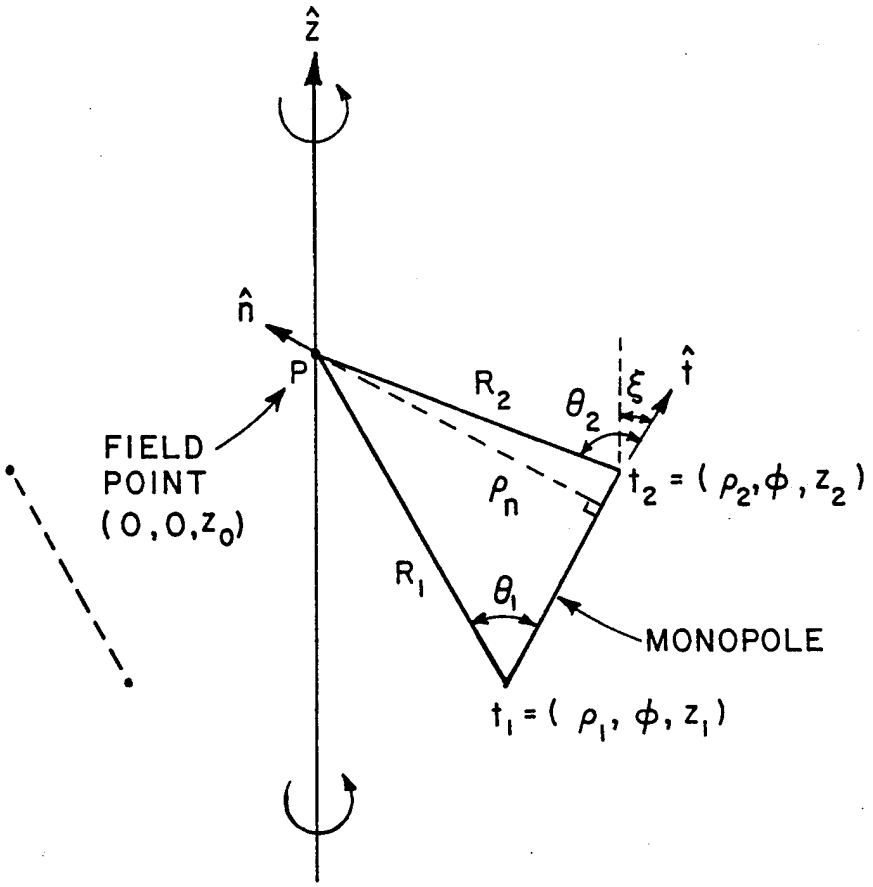

Figure 2.4. Geometry for the radiation of a monopole with end points t_1, t_2 and the field point 0 on the axis of revolution.

The vector potential $\vec{A}_1$ is given by

$$\vec{A}_1 = \int_S \hat{t}\, J_1^t \frac{e^{-jkR}}{4\pi R}\, ds'$$

$$= \int_0^{2\pi} \int_{t_1}^{t_2} \hat{t}\, \frac{1}{k\rho(t')} \frac{I_1 \sin\left[k(t_2-t')\right] + I_2 \sin\left[k(t'-t_1)\right]}{\sin kd} \cos m\phi \cdot$$

$$\frac{e^{-jkR}}{4\pi R}\, \rho(t')\, dt'\, d\phi$$

or

$$\vec{A}_1 = \frac{1}{k}\int_0^{2\pi} \cos m\phi \left(\int_{t_1}^{t_2} \hat{t}\, \frac{I_1 \sin k(t_2-t') + I_2 \sin k(t'-t_1)}{\sin kd} \frac{e^{-jkR}}{4\pi R}\, dt' \right) d\phi$$

$$= \frac{1}{k} \int_0^{2\pi} \cos m\phi\, \vec{A}_1'\, d\phi$$

From the rotational symmetry of the problem, one can calculate the electric field $\vec{E}_1'$ associated with $\vec{A}_1'$ and then integrate over ϕ to find $\vec{E}_1$. The electric field $\vec{E}_1'$ radiated by

$$\vec{I}(t) = \hat{t}\, I(t) = \hat{t}\, \frac{I_1 \sin k(t_2-t') + I_2 \sin k(t'-t_1)}{\sin kd}$$

is similar to the radiation of a z-directed current element with the same current distribution. The cylindrical components of the field are given as [3]

$$E_t = \frac{\eta}{4\pi j \sin kd}\left[\left(I_1 - I_2 \cos kd\right)\frac{e^{-jkR_2}}{R^2} + \left(I_2 - I_1 \cos kd\right)\frac{e^{-jkR_1}}{R^2}\right]$$

and

$$E_n = \frac{\eta}{4\pi j\ \rho_n \sin kd}\left[\left(I_1\, e^{-jkR_1} - I_2\, e^{-jkR_2}\right) j \sin kd\right.$$

$$\left. + (I_1 \cos kd - I_2)e^{-jkR_1} \cos\theta_1 + (I_2 \cos kd - I_1)e^{-jkR_2} \cos\theta_2\right]$$

where η is the free space wave impedance and E_t is the component along the axis of the monopole and E_n is the component orthogonal to the axis. The electric field $\vec{E}_1'$ is thus given by

$$\vec{E}_1' = \hat{t}\, E_t + \hat{n}\, E_n \qquad , z_o > z_c$$

or

$$\vec{E}_1' = \hat{t}\, E_t + \hat{n}'\, E_n$$

$$= \hat{t}\, E_t - \hat{n}\, E_n \qquad , z_o < z_c$$

as shown in Figure 2.5.

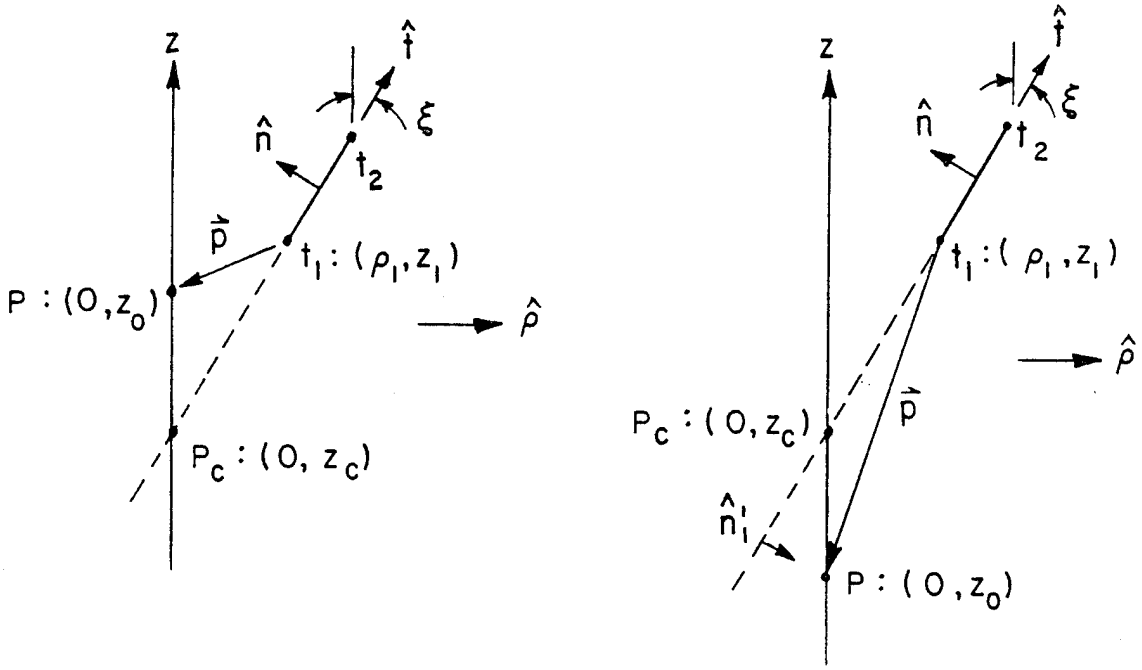

Figure 2.5. Geometry for the discussion of normal component E_n.

From Figure 2.2,

$$\hat{t} \times \vec{p} = \left(\hat{\rho} \sin\xi + \hat{z} \cos\xi\right) \times \left(-\hat{\rho}\rho_1 + \hat{z}(z_o - z_1)\right)$$

$$= \left[-(z_o - z_1)\sin\xi - \rho_1 \cos\xi\right]\hat{\phi}$$

$$= -\left[(z_o - z_1)\sin\xi + \rho_1 \cos\xi\right]\hat{\phi} \ .$$

When $z_o > z_c$, $\hat{t} \times \vec{p}$ is in the $-\hat{\phi}$ direction so that $\left[(z_o - z_1)\sin\xi + \rho_1\cos\xi\right] > 0$; when $z_o < z_c$, $\hat{t} \times \vec{p}$ is in the $\hat{\phi}$ direction so that $\left[(z_o - z_1)\sin\xi + \rho_1\cos\xi\right] < 0$. Consequently, the electric field $\vec{E}_1'$ can be written as

$$\vec{E}_1' = \hat{t}\, E_t + \text{sgn}[(z_o - z_1)\sin\xi + \rho_1\cos\xi]\, \hat{n}\, E_n$$

or

$$\vec{E}_1' = (\hat{\rho} \sin\xi + \hat{z} \cos\xi)E_t + \text{sgn}[(z_o - z_1)\sin\xi + \rho_1\cos\xi] \cdot$$

$$(-\hat{\rho} \cos\xi + \hat{z} \sin\xi)\, E_n$$

or

$$\vec{E}_1' = \hat{\rho}\left\{\sin\xi\ E_t - \mathrm{sgn}[(z_o-z_1)\sin\xi + \rho_1\cos\xi]\ \cos\xi\ E_n\right\}$$

$$+ \hat{z}\left\{\cos\xi\ E_t + \mathrm{sgn}[(z_o-z_1)\sin\xi + \rho_1\cos\xi]\ \sin\xi\ E_n\right\}$$

$$= \left(\hat{x}\cos\phi + \hat{y}\sin\phi\right)\left\{\sin\xi\ E_t - \mathrm{sgn}[(z_o-z_1)\sin\xi + \rho_1\cos\xi]\ \cos\xi\ E_n\right\}$$

$$+ \hat{z}\left\{\cos\xi\ E_t + \mathrm{sgn}[(z_o-z_1)\sin\xi + \rho_1\cos\xi]\ \sin\xi\ E_n\right\}$$

Consequently,

$$\vec{E}_1(0,0,z_o) = \frac{1}{k}\int_0^{2\pi} \cos m\phi\ \vec{E}_1'(0,0,z)\ d\phi$$

or

$$\vec{E}_1(0,0,z_o) = \begin{cases} 0 & , \ m>1 \\ \hat{x}\ \frac{\pi}{k}\left\{\sin\xi\ E_t + \mathrm{sgn}[(z_o-z_1)\sin\xi + \rho_1\cos\xi]\ \cos\xi\ E_n\right\}, & m=1 \\ \hat{z}\ \frac{2\pi}{k}\left\{\cos\xi\ E_t + \mathrm{sgn}[(z_o-z_1)\sin\xi + \rho_1\cos\xi]\sin\xi\ E_n\right\}, & m=0 \end{cases}$$

Thus, the excitation element V_1^t is given by

$$V_1^t = \hat{x}\ P_x \cdot \vec{E}_1(0,0,z_o)$$

$$= P_x\ \frac{\pi}{k}\left\{E_t\ \sin\xi - \mathrm{sgn}[(z_o-z_1)\sin\xi + \rho_1\cos\xi]E_n\ \cos\xi\right\}\ ,\ m=1 \qquad (17)$$

In Equation (17), P_x is the dipole strength of the primary source, the function sgn(x) is defined as

$$\text{sgn}(x) = \pm 1, \text{ if } x \gtrless 0,$$

and $(0,z_o)$ and (ρ_1,z_1) are the coordinates of the point P and t_1.

The excitation element V_1^ϕ associated with the current mode $\hat{\phi}\, J_1^\phi$ is obtained accordingly by the equation

$$V_1^\phi = \int_S \hat{\phi}\, J_1^\phi \cdot \vec{E}^i \, ds$$

$$= -j\omega \int_S \left[\hat{\phi}\, J_1^\phi \cdot \vec{A}^i - \frac{1}{k^2}\left(\nabla \cdot \hat{\phi}\, J_1^\phi\right)\left(\nabla \cdot \vec{A}^i\right)\right] ds \qquad (18)$$

The vector potential due to a perpendicular on-axis dipole is

$$\vec{A}^i = \hat{x}\, P_x \frac{\mu_o e^{-jkR}}{4\pi R} \qquad (19)$$

where R is the distance from the on-axis dipole to the current J_1^ϕ. The current J_1^ϕ is given by

$$\hat{\phi}\, J_1^\phi = \hat{\phi}\left[I_1^\phi P_1(t) + I_{1+1}^\phi P_{1+1}(t)\right]\sin m\phi \, .$$

In view of the form of J_1^ϕ, the excitation element associated with the current mode $P_1(t) \sin m\phi$ is discussed next.

From Equation (18), the excitation element associated with $\hat{\phi}\, P_1(t) \sin m\phi$ is given by

$$V_1^{\phi} = - j\omega \int_S \left\{ \hat{\phi}\, P_1(t) \sin m\phi \cdot \vec{A}^i - \frac{1}{k^2} \left[\nabla \cdot (\hat{\phi}\, P_1(t) \sin m\phi) \right] \left(\nabla \cdot \vec{A}^i \right) \right\} dS$$

where

$$\hat{\phi} \cdot \vec{A}^i = \hat{\phi} \cdot \hat{x}\, P_x \frac{\mu_o\, e^{-jkR}}{4\pi R} = - \sin\phi\, P_x \frac{\mu_o\, e^{-jkR}}{4\pi R} \quad ,$$

$$\nabla \cdot (\hat{\phi}\, P_1(t) \sin m\phi) = \frac{1}{\rho} \frac{\partial}{\partial \phi} (P_1(t) \sin m\phi) = \frac{m}{\rho} P_1(t) \cos m\phi \quad ,$$

and

$$\nabla \cdot \vec{A}^i = \nabla \cdot \left(\hat{x}\, P_x \frac{\mu_o\, e^{-jkR}}{4\pi R} \right)$$

$$= P_x \frac{\mu_o}{4\pi} \frac{\partial}{\partial x} \left(\frac{e^{-jkR}}{R} \right)$$

$$= \frac{\mu_o P_x}{4\pi} \frac{\partial}{\partial R} \left(\frac{e^{-jkR}}{R} \right) \frac{\partial R}{\partial x}$$

$$= \frac{\mu_o P_x}{4\pi} \left(- \frac{jk}{R} e^{-jkR} - \frac{e^{-jkR}}{R^2} \right) \frac{x - x'}{R} \quad .$$

For the on-axis dipole, $x'=0$ and $x=\rho \cos\phi$ so that $\nabla \cdot \vec{A}^i$ becomes

$$\nabla \cdot \vec{A}^i = \frac{\mu_o P_x}{4\pi} \left(- \frac{jk}{R} - \frac{1}{R^2} \right) \frac{e^{-jkR}}{R} \rho \cos\phi \ .$$

Substituting the above relations into V_1^ϕ, the following equation is obtained:

$$V_1^\phi = - j\omega \int_S \Big\{ - P_x P_1(t) \frac{\mu_o e^{-jkR}}{4\pi R} \sin\phi \sin m\phi$$

$$- \frac{1}{k^2} \left(\frac{m}{\rho} P_1(t) \cos m\phi \right) \left[\frac{\mu_o P_x}{4\pi} \left(- \frac{jk}{R} - \frac{1}{R^2} \right) \right] \frac{e^{-jkR}}{R} \rho \cos\phi \Big\} dS$$

$$= \frac{j\omega\mu_o}{4\pi k^2} P_x \int_0^{2\pi} \int_t P_1(t) \Big\{ k^2 \sin\phi \sin m\phi - m \left(\frac{jk}{R} + \frac{1}{R^2} \right) \cos m\phi \cos\phi \Big\} \frac{e^{-jkR}}{R} \rho dt d\phi$$

The integration over ϕ results in

$$\int_0^{2\pi} \sin\phi \sin m\phi \, d\phi = \begin{cases} 0 \ , & m \neq 1 \\ \pi \ , & m = 1 \end{cases}$$

and

$$\int_0^{2\pi} \cos\phi \cos m\phi \, d\phi = \begin{cases} 0 \ , & m \neq 1 \\ \pi \ , & m = 1 \end{cases} \ .$$

For the horn radiation problem, m=1, and V_1^ϕ becomes

$$V_1^\phi = \frac{j\omega\mu_o}{4k^2} P_x \int_t P_1(t) \left(k^2 - \frac{jk}{R} - \frac{1}{R^2} \right) \frac{e^{-jkR}}{R} \rho \, dt \qquad (20)$$

The complete V_1^{ϕ} is then the sum of two such equations (Equation (20)) associated with the two current modes comprising the current $J_1^{\phi}\,\hat{\phi}$.

C. Far Zone Fields

The vector potential in the far-field zone due to a current mode of Equation (5) is given by

$$\vec{A}_n = \frac{\mu_o e^{-jkr}}{4\pi r} \int \vec{J}_n \, e^{jk\hat{r}\cdot\vec{r}'} \, \rho' dt' d\phi'$$

$$= \frac{\mu_o e^{-jkr}}{4\pi r} \int \left[\hat{t}' \cos m\phi \, I_n^t \frac{Q_n(t')}{k\rho'} + \hat{\phi}' \sin m\phi \, I_n^{\phi} P_n(t') \right]$$

$$\cdot \, e^{jk[\rho' \sin\theta \cos(\phi'-\phi) + z'\cos\theta]} \, \rho' \, dt' \, d\phi' \qquad (21)$$

In view of the relations (excluding the $\hat{r}$ component)

$$\hat{\phi}' = \hat{\phi} \cos(\phi'-\phi) - \hat{\theta} \sin(\phi'-\phi) \cos\theta \qquad (22)$$

$$\hat{t}' = \hat{\phi} \sin\xi' \sin(\phi'-\phi) + \hat{\theta}[\sin\xi' \cos\theta \cos(\phi'-\phi) - \cos\xi' \sin\theta] \, . \qquad (23)$$

Equation (21) then reduces to

$$A_{n\phi}^{\phi} = \frac{\mu_o e^{-jkr}}{2\,r} I_n^{\phi} \sin m\phi \, j^{m-1} \int J_m'(k\rho' \sin\theta) P_n(t') e^{jkz'\cos\theta} \rho' dt'$$

$$A^{\phi}_{n\theta} = \frac{-\mu_o e^{-jkr}}{2\,r}\, I^{\phi}_n \cos m\phi\; j^{m-1} \int \frac{m\cos\theta}{k\rho'\sin\theta}\, J_m(k\rho'\sin\theta) P_n(t') e^{jkz'\cos\theta} \rho' dt'$$

$$A^{t}_{n\phi} = \frac{-\mu_o e^{-jkr}}{2\,r}\, \frac{I^{t}_n}{k} \sin\xi' \sin m\phi\; j^{m-1} \int \frac{m}{k\rho'\sin\theta} J_m(k\rho'\sin\theta) Q_n(t') e^{jkz'\cos\theta} dt'$$

$$A^{t}_{n\theta} = \frac{\mu_o e^{-jkr}}{2\,r}\, \frac{I^{t}_n}{k} \cos m\phi\; j^{m-1} \int [J'_m(k\rho'\sin\theta) \sin\xi'\cos\theta$$

$$- j\cos\xi' \sin\theta\, J_m(k\rho'\sin\theta)] Q_n(t') e^{jkz'\cos\theta} dt' \qquad (24)$$

where J_m is a Bessel function and J'_m is its derivative with respect to the argument.

For the radiated field of a conical horn antenna, one also needs to include the radiation due to the primary dipole source. In the far-field zone, the vector potential of the perpendicular on-axis dipole of strength P_x is

$$\vec{A} = (\hat{\theta}\cos\theta\cos\phi - \hat{\phi}\sin\phi)\, \frac{\mu_o P_x}{4\pi r}\, e^{-jkr + jkz_o\cos\theta} \,. \qquad (25)$$

The total radiated field can then be obtained from (24) and (25) as

$$\begin{cases} E_\theta = -j\omega\mu_o A_{\theta,\text{total}} \\ E_\phi = -j\omega\mu_o A_{\phi,\text{total}} \end{cases} .$$

III. EXAMPLES

In this section, six horn antennas are used as examples to validate the moment method computer code. The calculated patterns are compared with the measured patterns.

A. Prime Focus Conical Horn

The geometry of this horn antenna is shown in Figure 3.1. The radiation patterns of this horn, calculated at 11 GHz, are shown in Figure 3.2. The measured patterns are given in Figure 3.3 for comparison.

B. Prime Focus Corrugated Horn

The geometry of this corrugated horn is given in Figure 3.4. The inner dimension of this horn is used as a conical horn and the H-plane pattern of this simulated conical horn is calculated at 11.0 GHz. The resulting pattern, which is given in Figure 3.5, is treated as the pattern of the corrugated horn and assumed circularly symmetric. The measured principal plane patterns are shown in Figure 3.6.

C. Prime Focus Dual-Mode Horn

The geometry of this horn is shown in Figure 3.7. The moment method calculated patterns are shown in Figure 3.8 with the measured patterns shown in Figure 3.9.

D. Conical Horn for Cassegrain Reflector

The geometry for this horn antenna is shown in Figure 3.10. The radiation patterns of this horn, calculated at 11.0 GHz, are shown in Figure 3.11. The measured patterns are given in Figure 3.12 for comparison.

E. Corrugated Horn for Cassegrain Reflector

The geometry of this corrugated horn is given in Figure 3.13. The inner dimension of this horn is used as a conical horn and the H-plane pattern of this simulated conical horn is calculated at 11.0 GHz. The resulting pattern, which is given in Figure 3.14, is treated as the pattern of the corrugated horn and assumed circularly symmetric. The measured principal plane patterns are shown in Figure 3.15.

F. Dual-Mode Horn for Cassegrain Reflector

The geometry of this horn is shown in Figure 3.16. The moment method calculated patterns are shown in Figure 3.17 with the measured patterns shown in Figure 3.18.

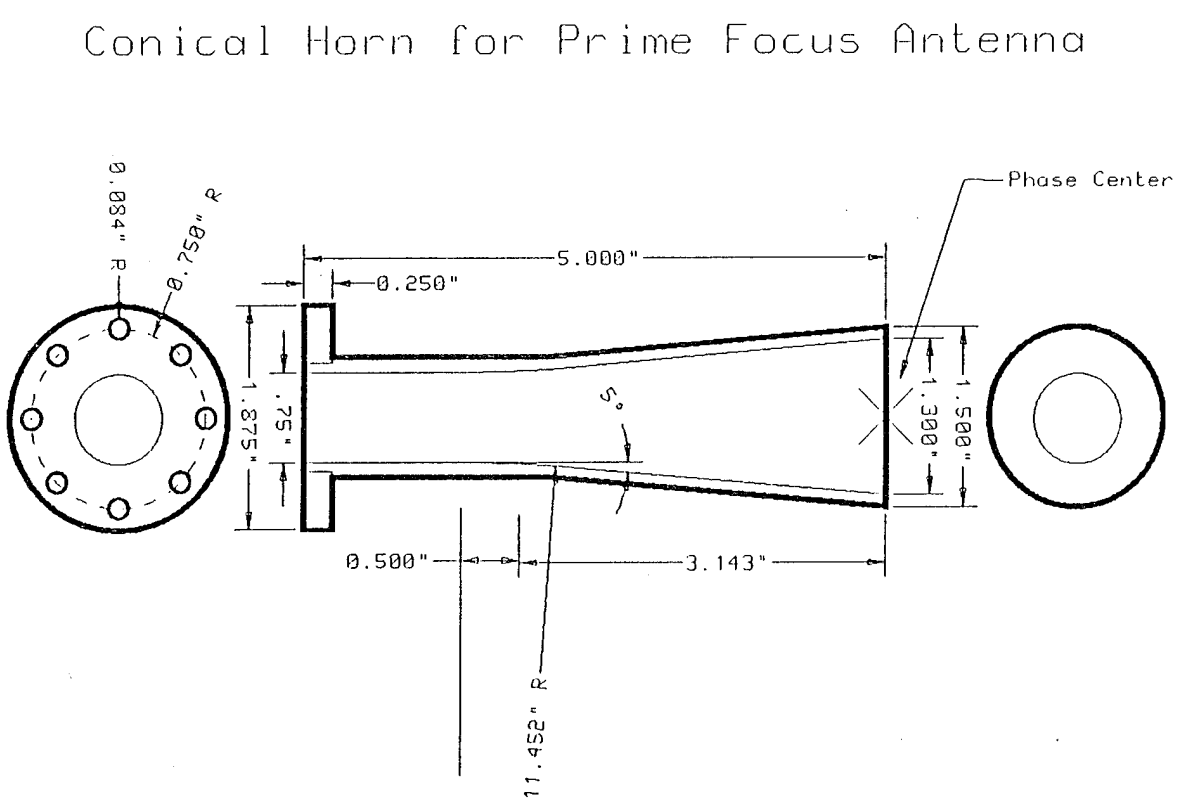

Figure 3.1(a). Geometry of the prime focus conical horn.

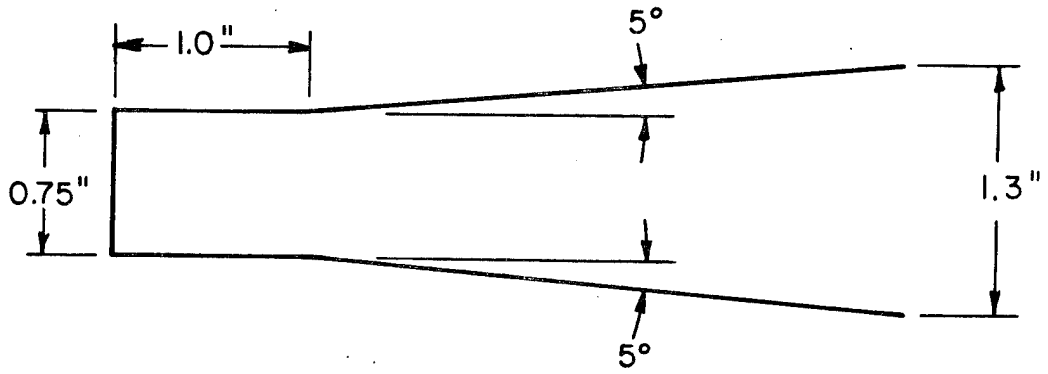

Figure 3.1(b). Equivalent geometry of the prime focus conical horn for moment method calculation.

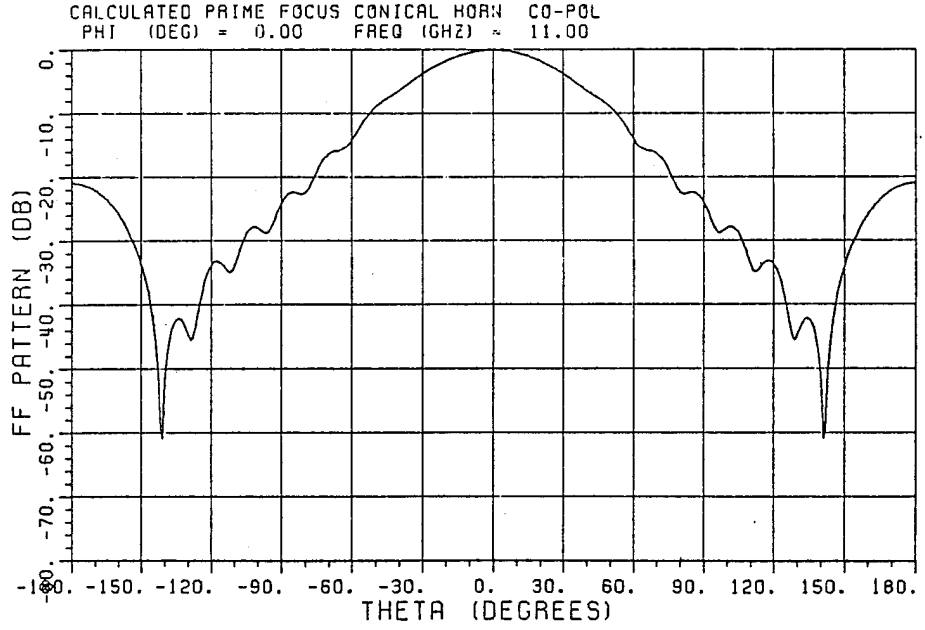

(a) H-plane

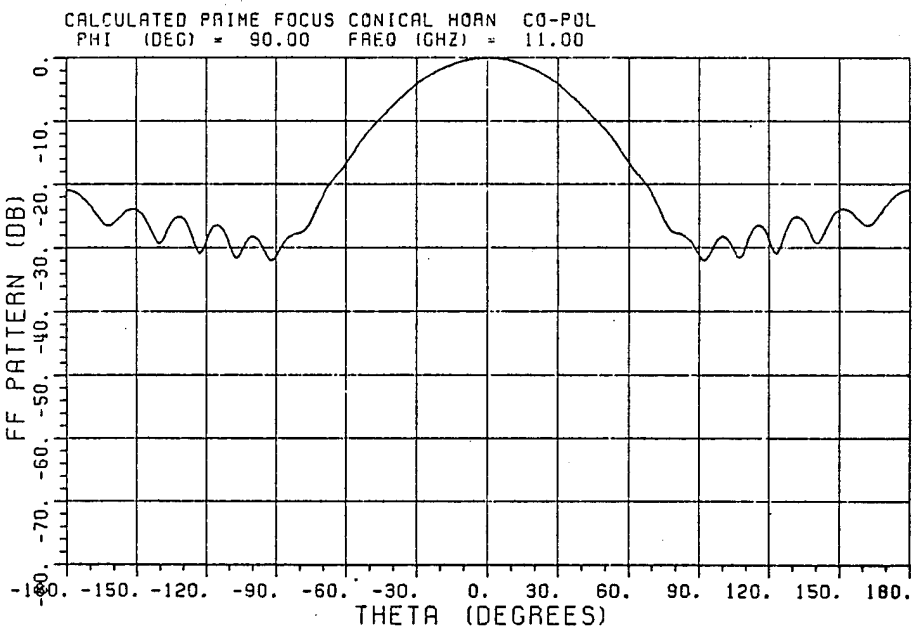

(b) E-plane

Figure 3.2. Calculated patterns of the prime focus conical horn at 11.0 GHz.

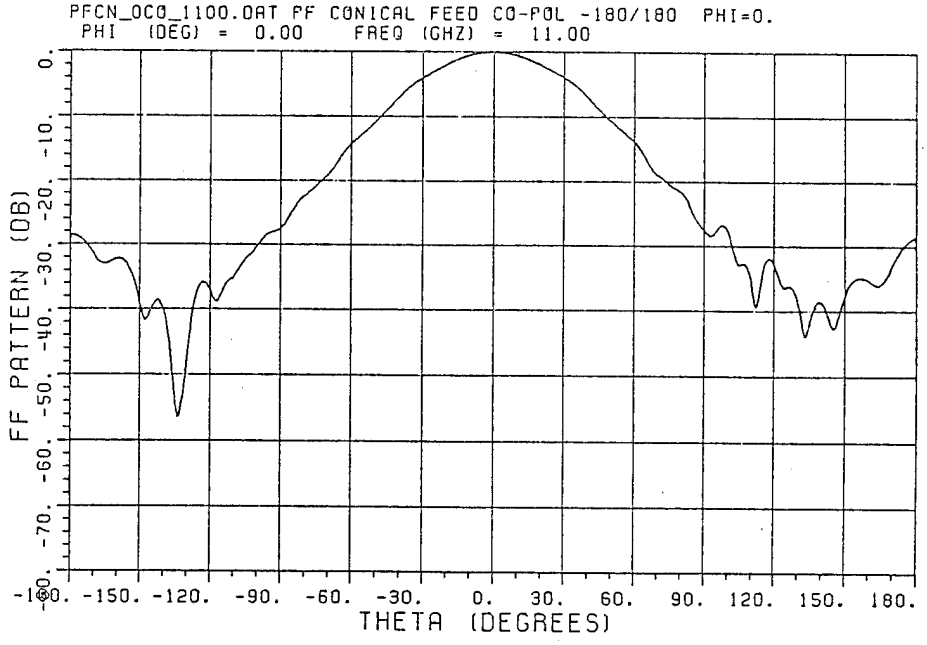

(a) H-plane

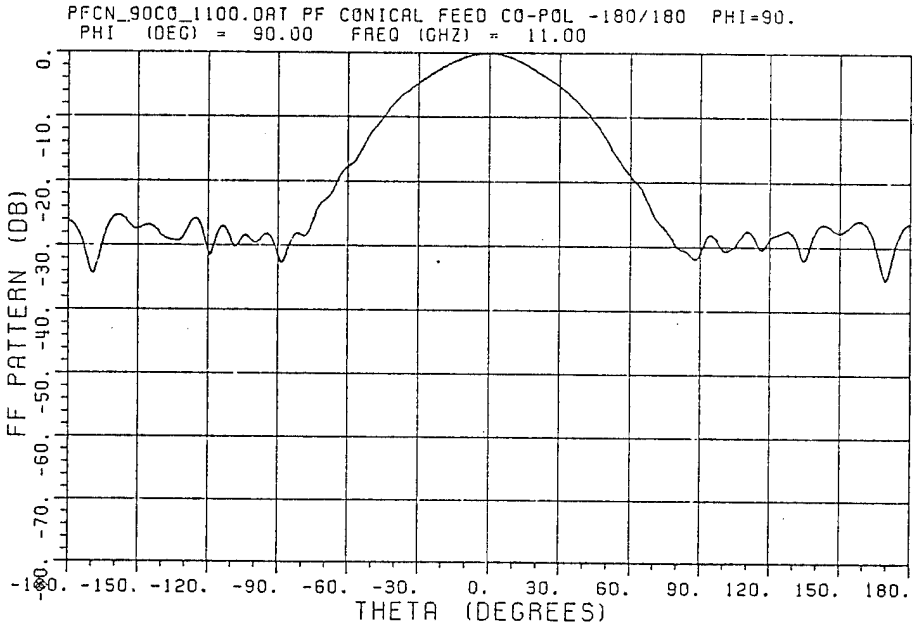

(b) E-plane

Figure 3.3. Measured patterns of the prime focus conical horn at 11.0 GHz.

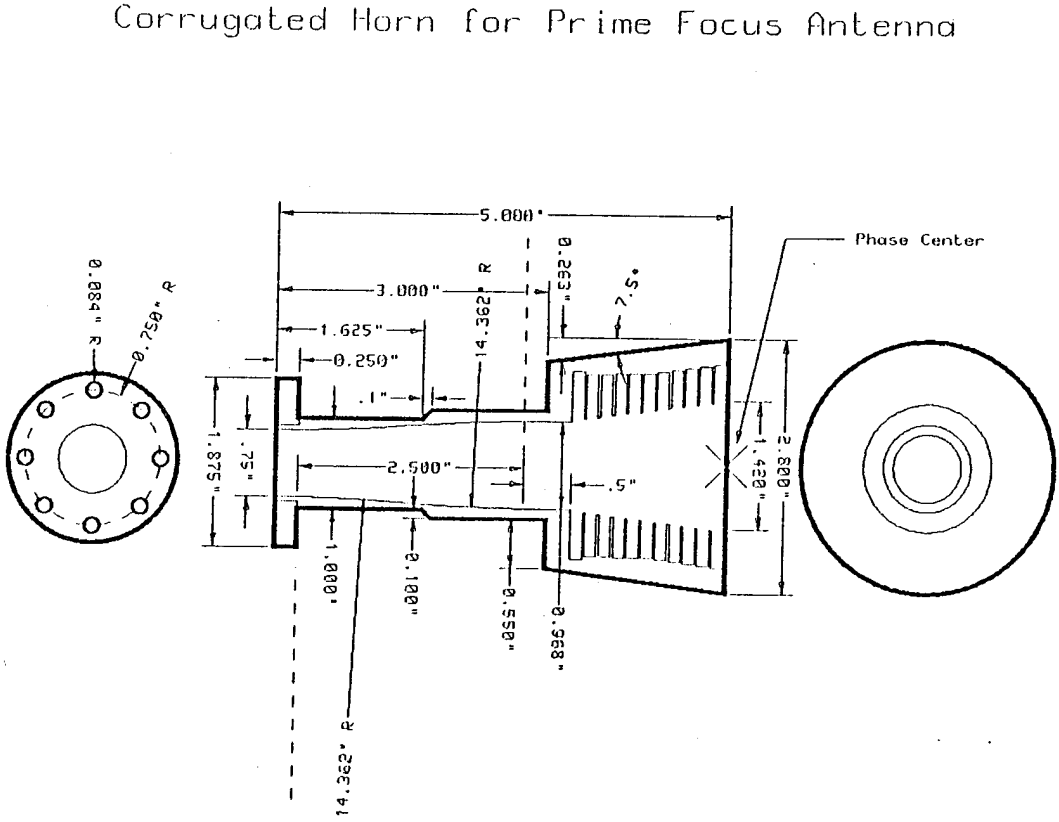

Figure 3.4(a). Geometry of the prime focus corrugated horn.

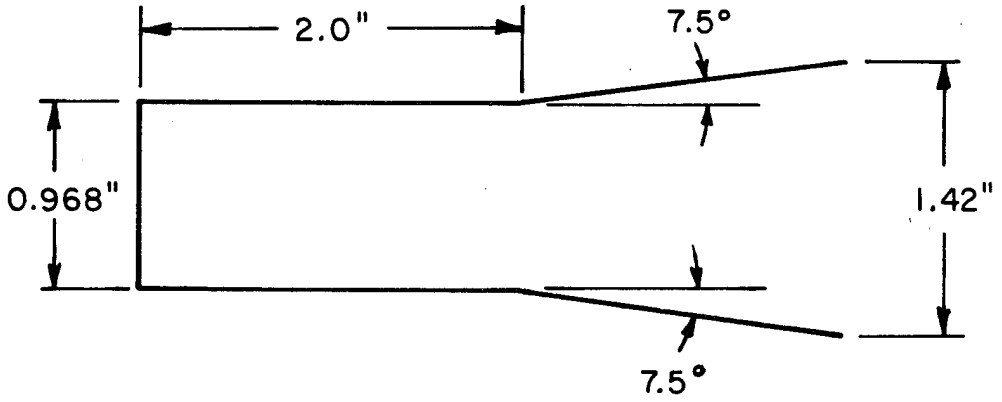

Figure 3.4(b). Equivalent conical horn of the prime focus corrugated horn for moment method calculation.

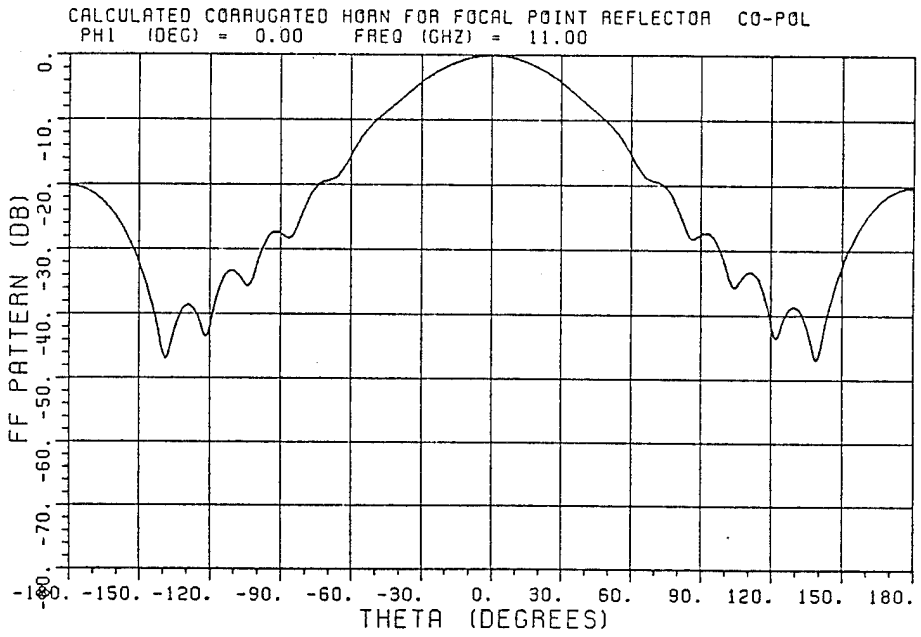

Figure 3.5. Calculated pattern of the prime focus corrugated horn at 11.0 GHz (simulated by a conical horn).

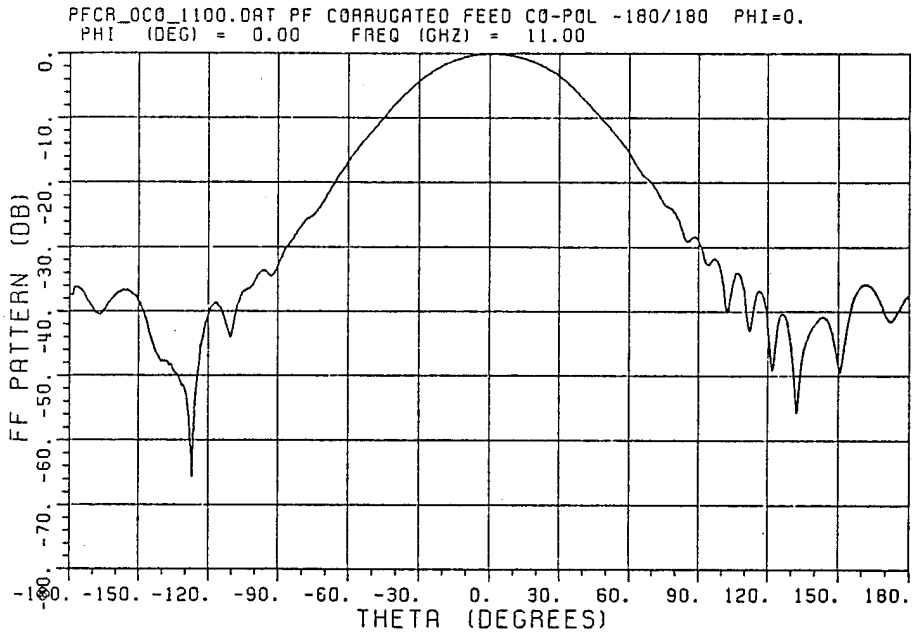

(a) H-plane

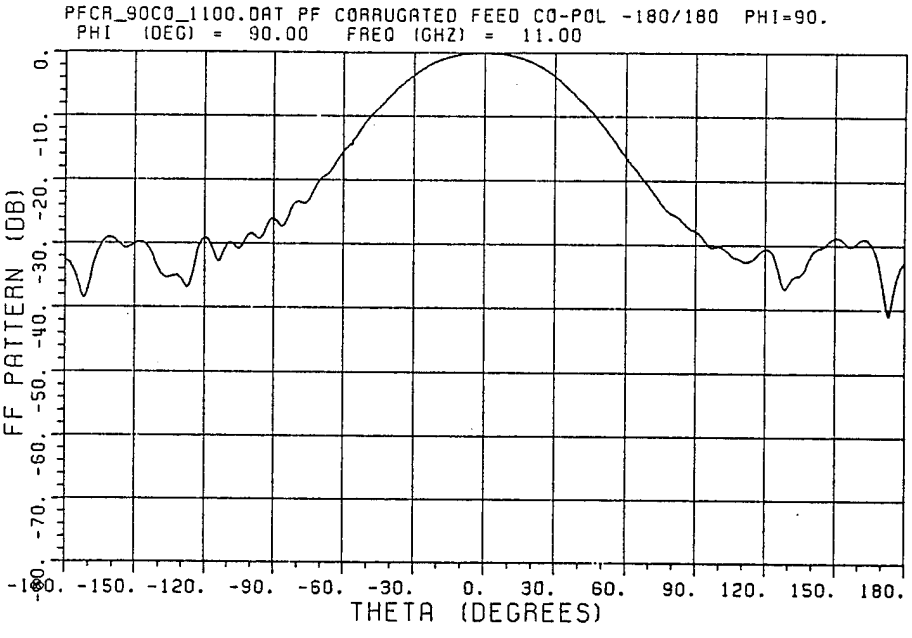

(b) E-plane

Figure 3.6. Measured patterns of the prime focus corrugated horn at 11.0 GHz.

Dual Mode Horn for Prime Focus Antenna

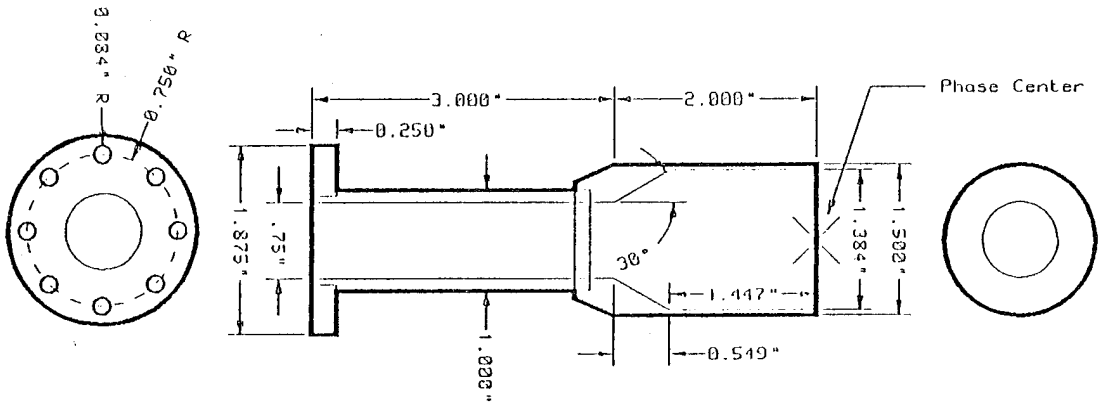

Figure 3.7(a). Geometry of the prime focus dual-mode horn.

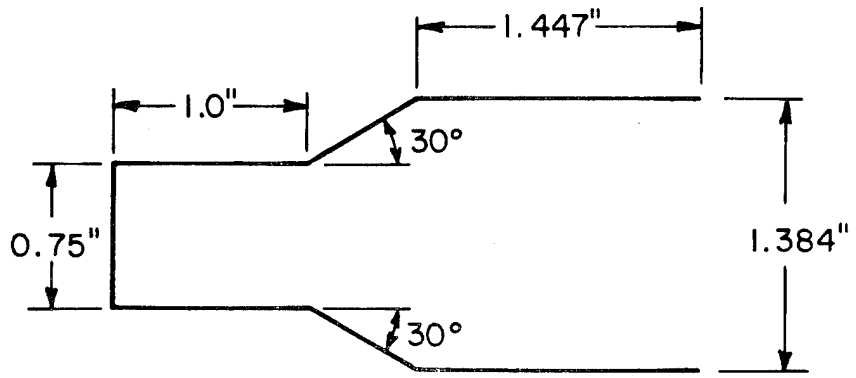

Figure 3.7(b). Equivalent geometry of the prime focus dual-mode horn for moment method calculation.

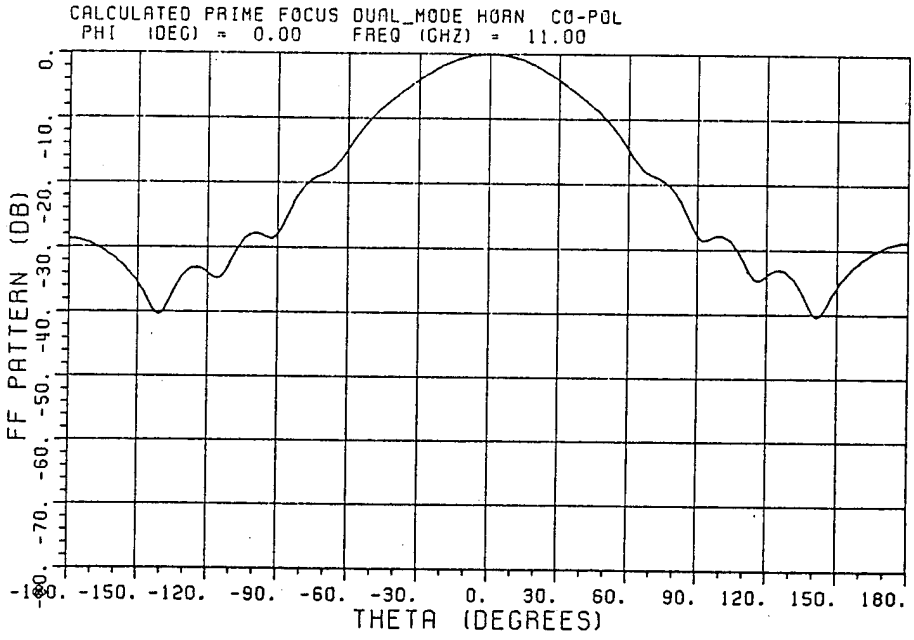

(a) H-plane

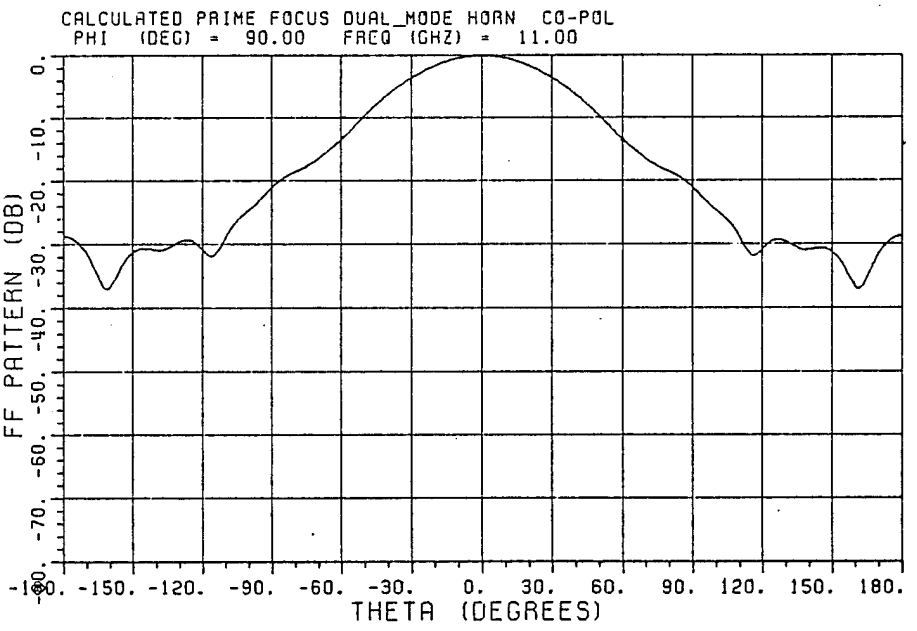

(b) E-plane

Figure 3.8. Calculated patterns of the prime focus dual-mode horn at 11.0 GHz.

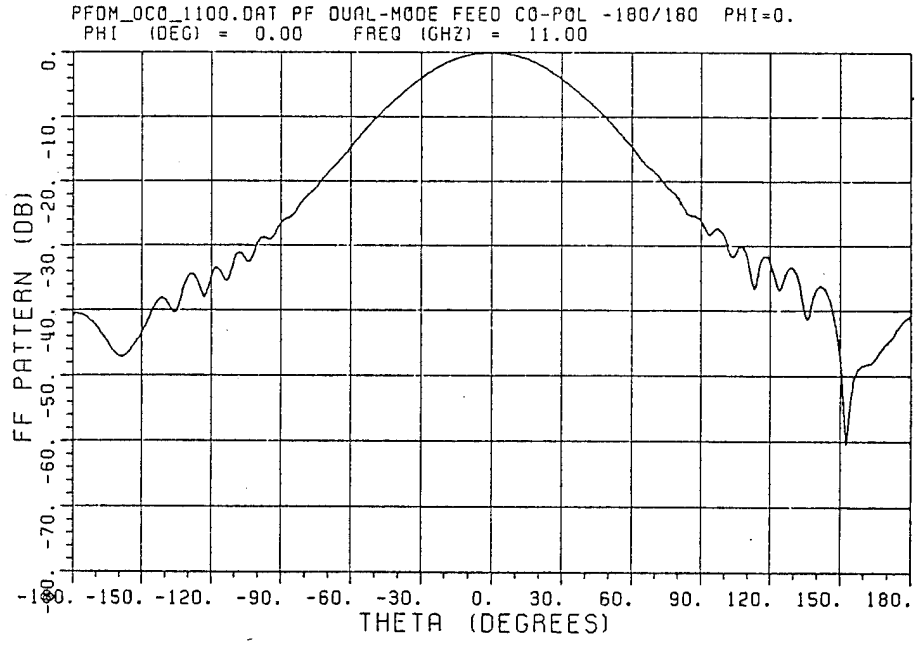

(a) H-plane

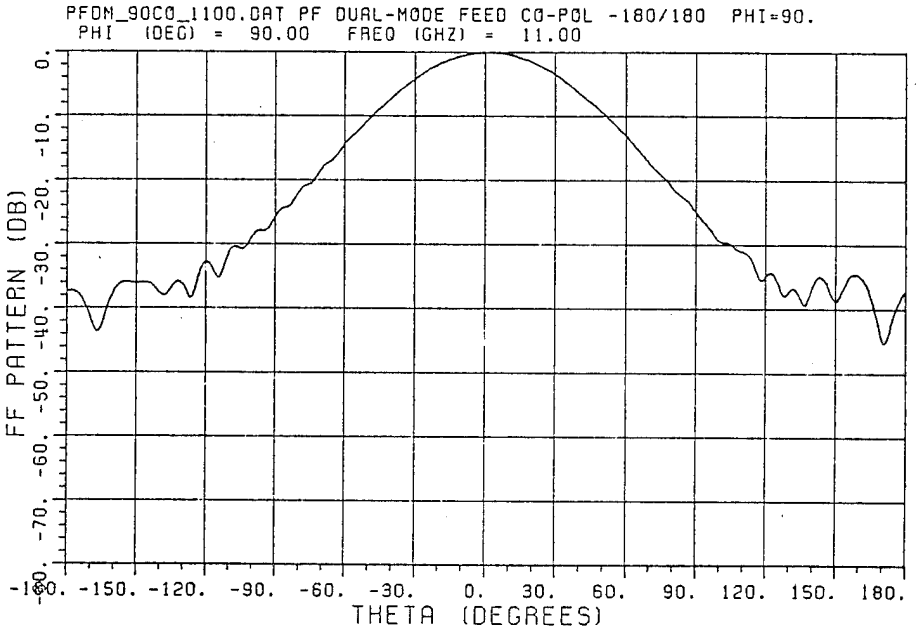

(b) E-plane

Figure 3.9. Measured patterns of the prime focus dual-mode horn at 11.0 GHz.

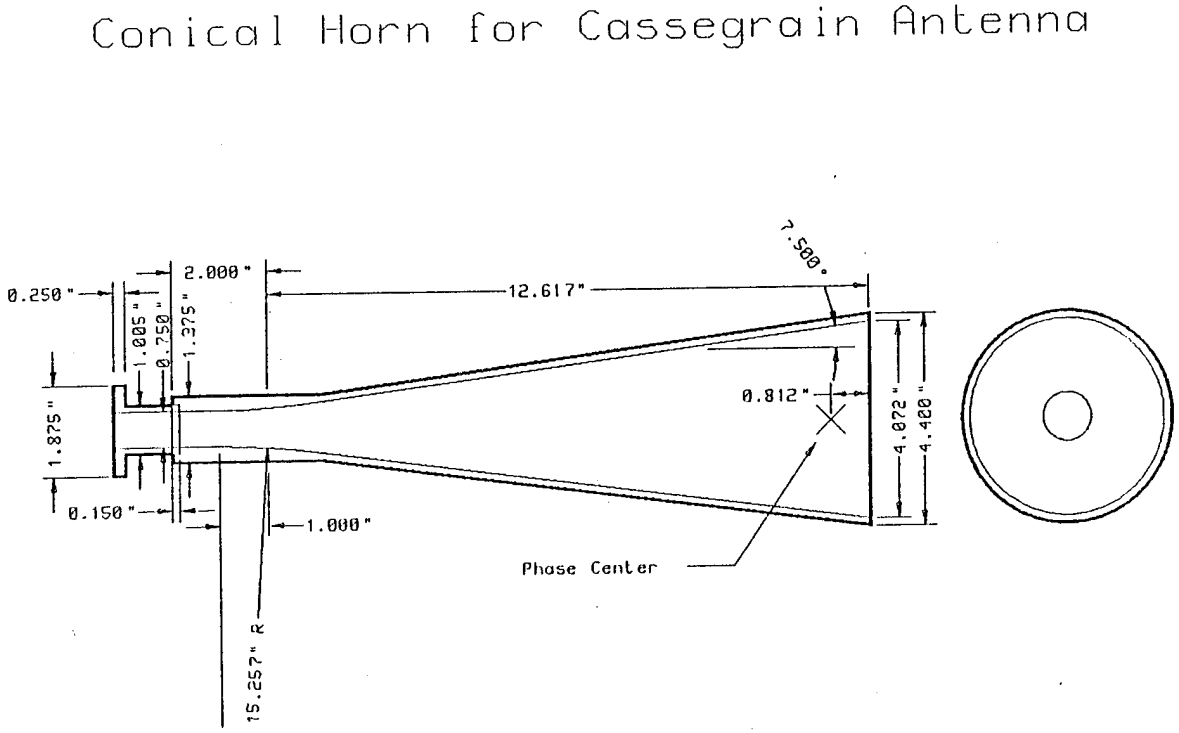

Figure 3.10(a). Geometry of the conical horn for Cassegrain reflector.

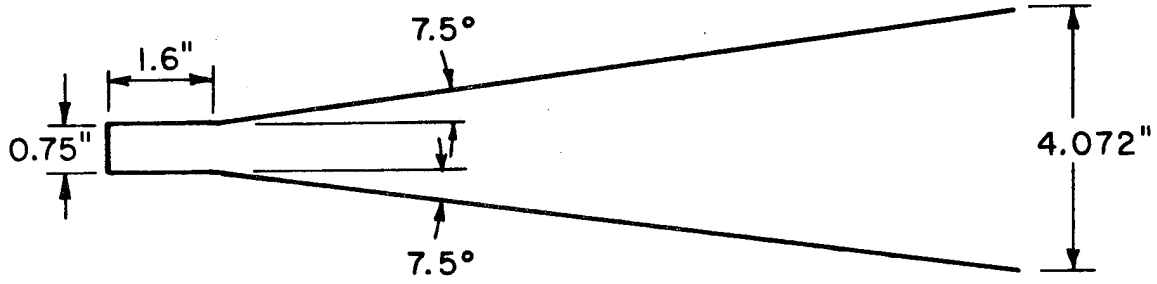

Figure 3.10(b). Equivalent geometry of the conical horn for Cassegrain reflector.

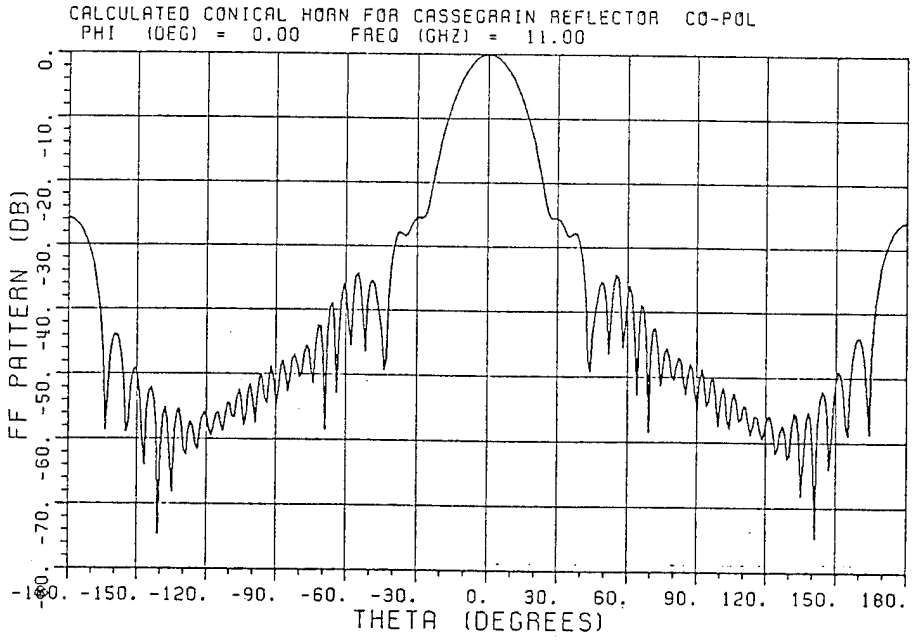

(a) H-plane

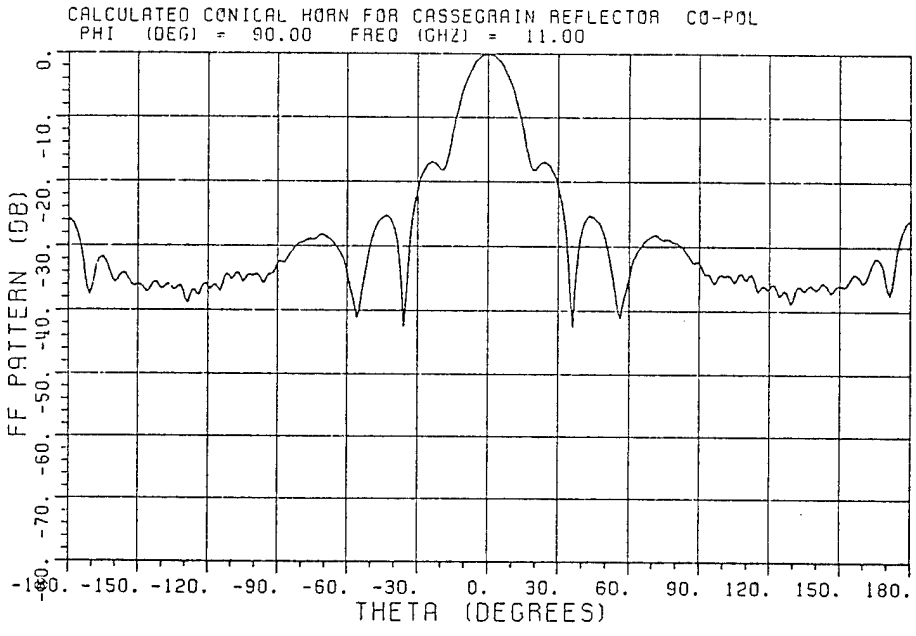

(b) E-plane

Figure 3.11. Calculated patterns of the conical horn for Cassegrain reflector at 11.0 GHz.

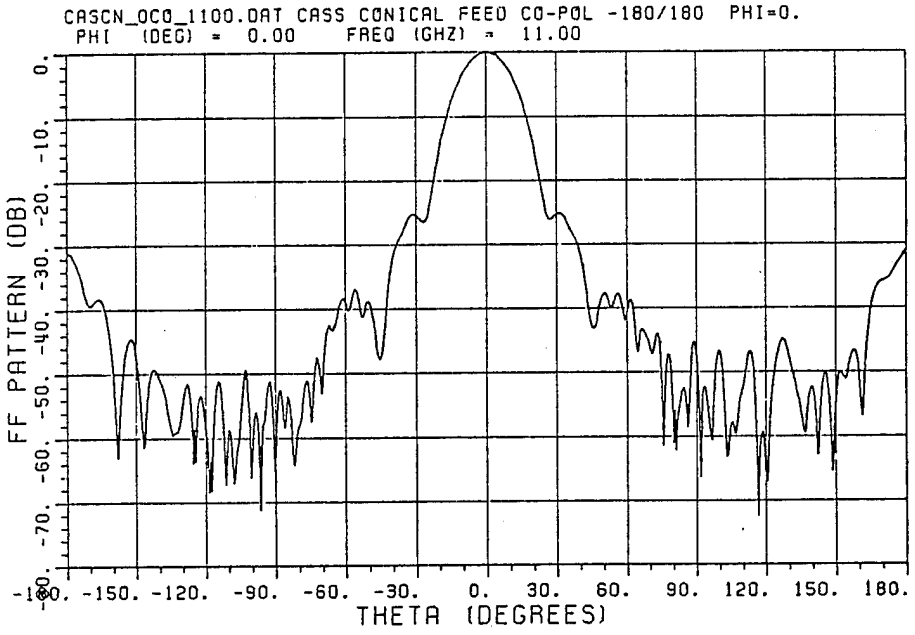

(a) H-plane

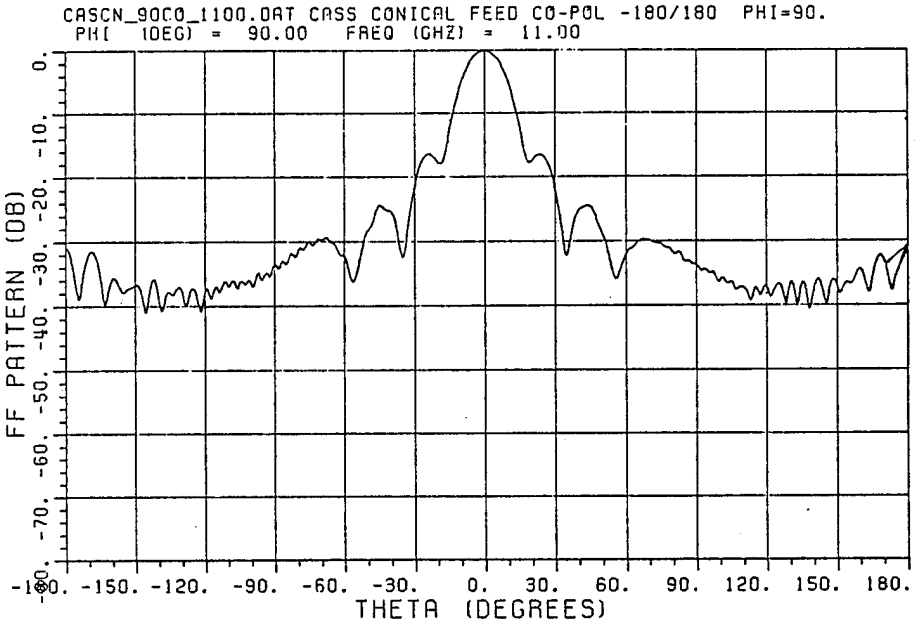

(b) E-plane

Figure 3.12. Measured patterns of the conical horn for Cassegrain reflector at 11.0 GHz.

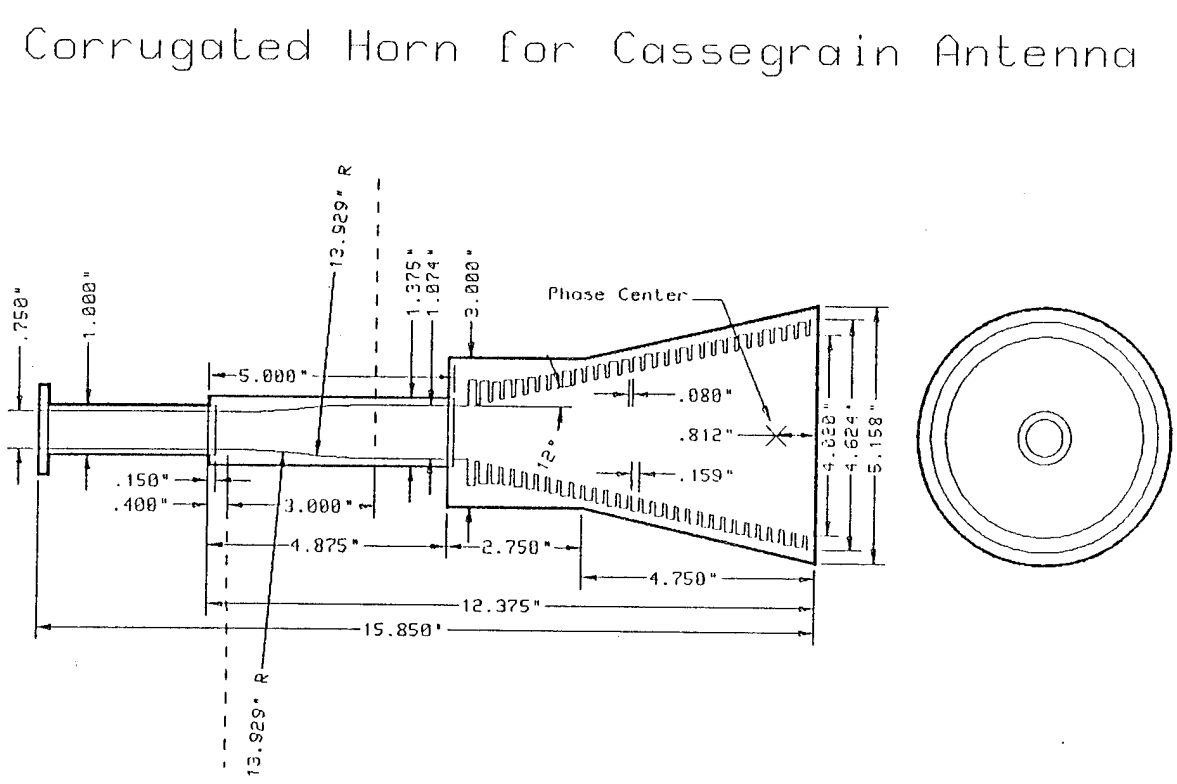

Figure 3.13(a). Geometry of the corrugated horn for Cassegrain reflector.

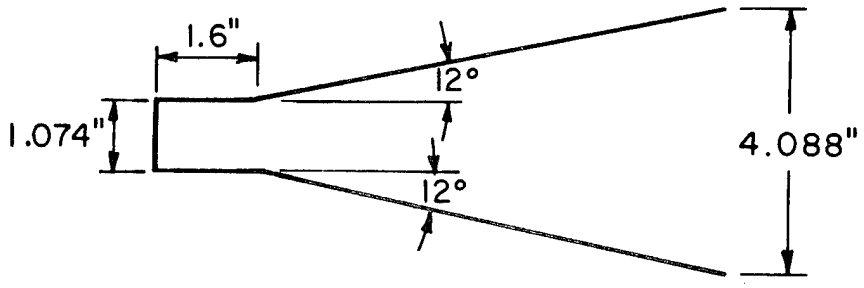

Figure 3.13(b). Equivalent conical horn of the corrugated horn for Cassegrain reflector.

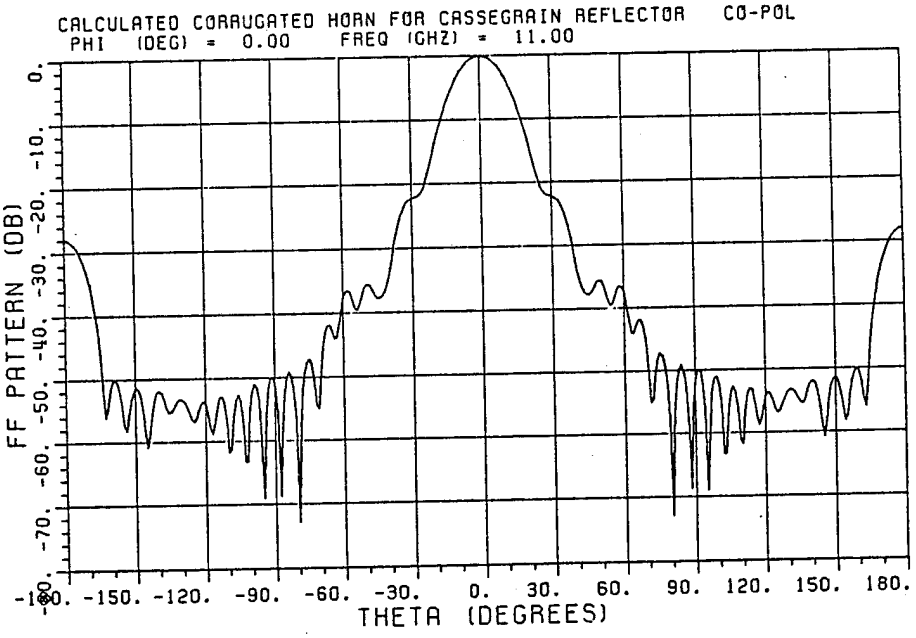

Figure 3.14. Calculated patterns of the corrugated horn for Cassegrain reflector at 11.0 GHz.

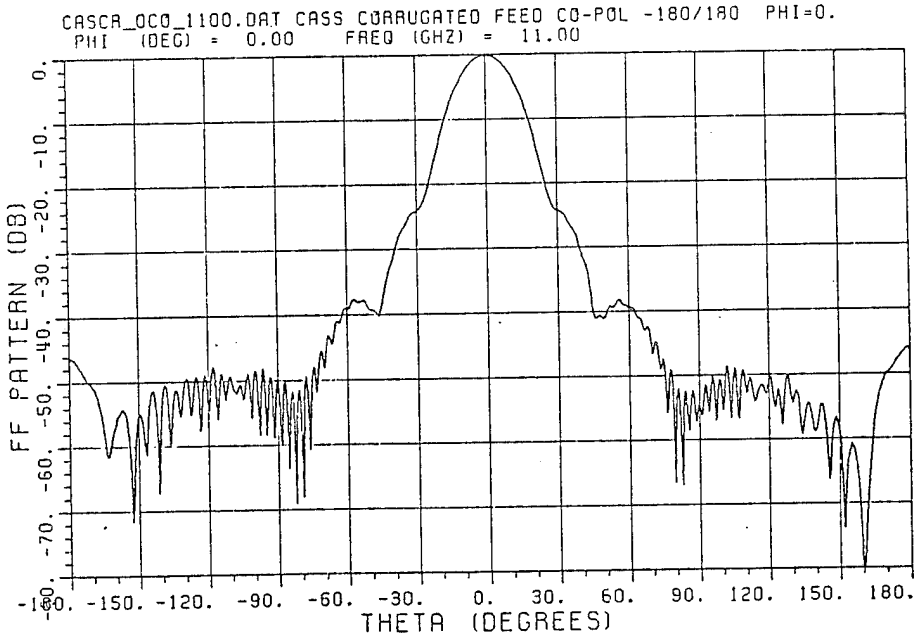

(a) H-plane

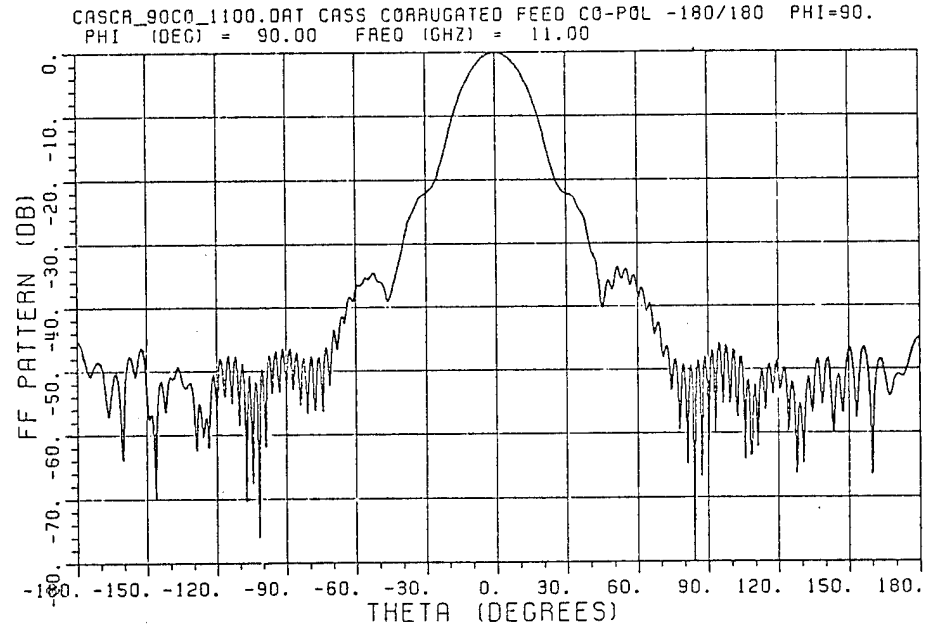

(b) E-plane

Figure 3.15. Measured patterns of the corrugated horn for Cassegrain reflector at 11.0 GHz.

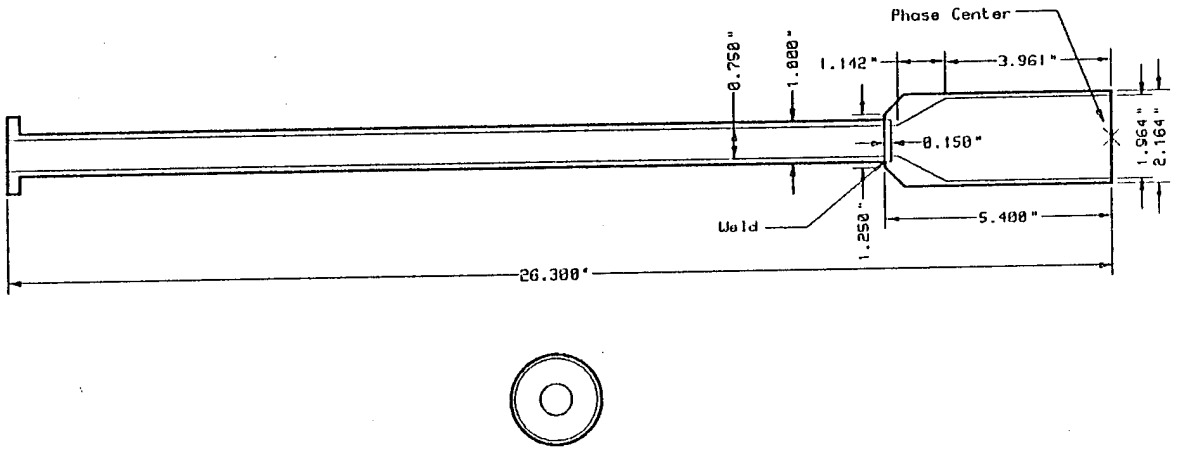

Figure 3.16(a). Geometry of the dual-mode horn for Cassegrain reflector.

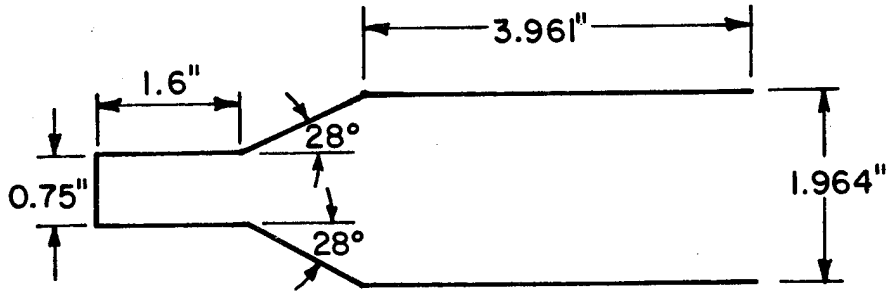

Figure 3.16(b). Equivalent geometry of the dual-mode horn for Cassegrain reflector.

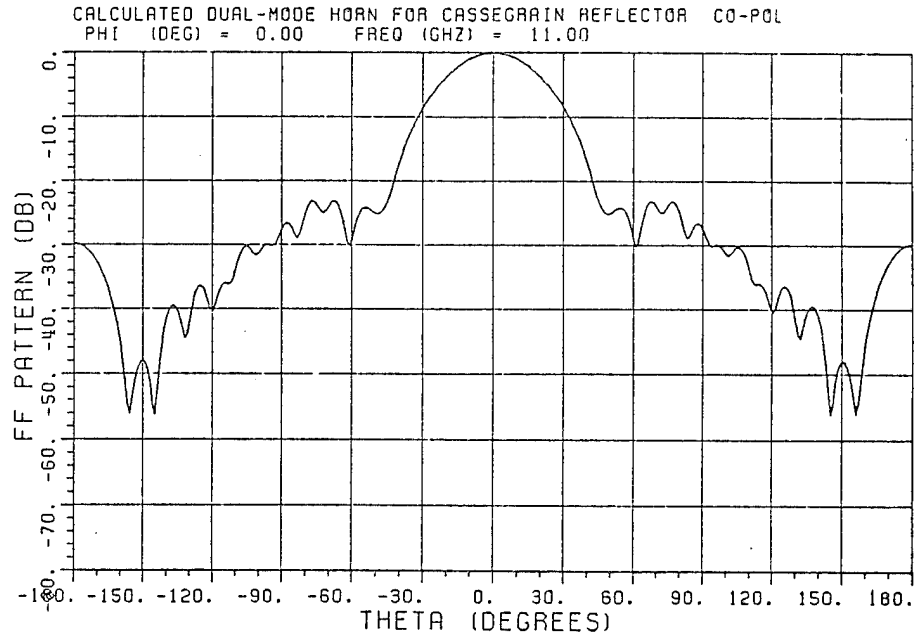

(a) H-plane

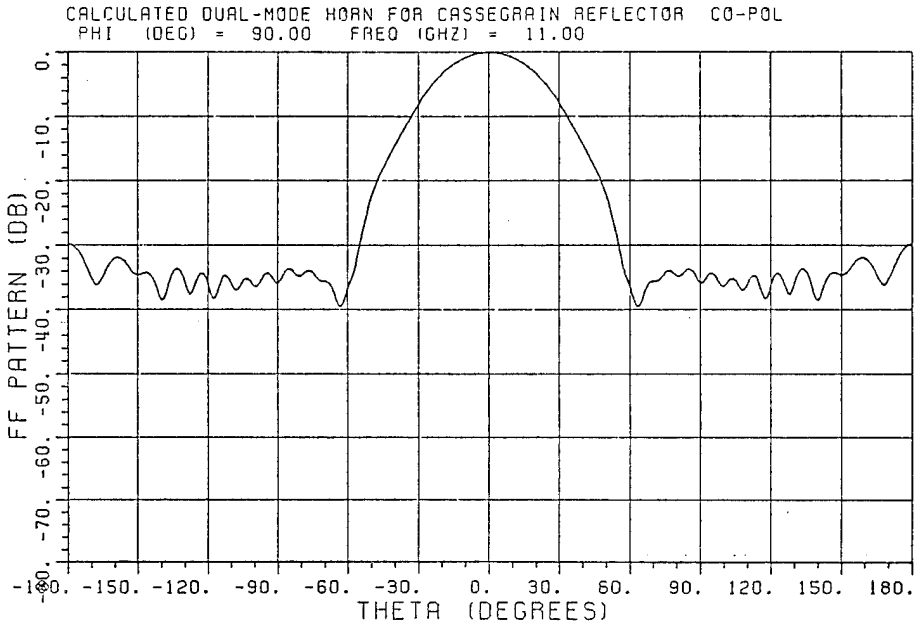

(b) E-plane

Figure 3.17. Calculated patterns of the dual-mode horn for Cassegrain reflector at 11.0 GHz.

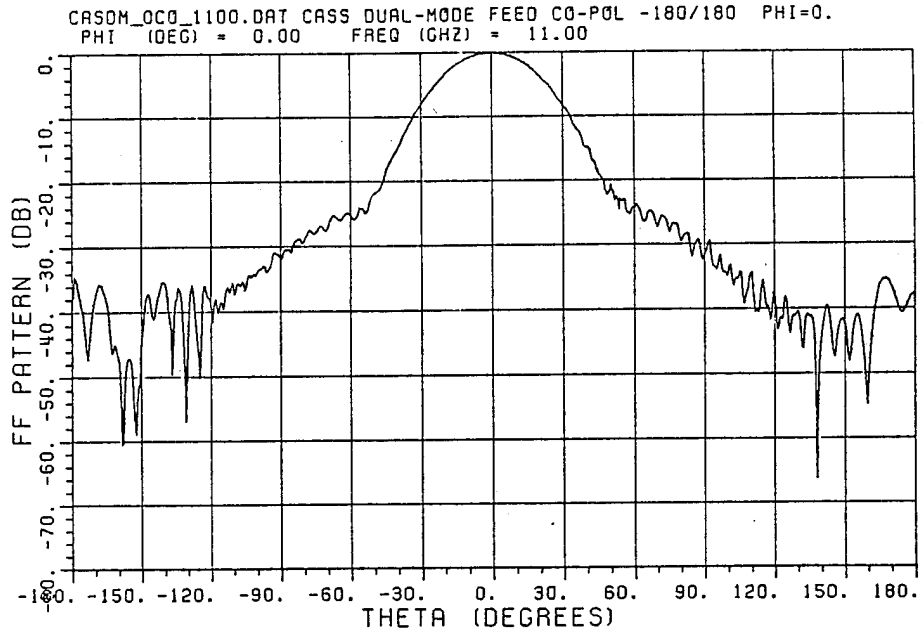

(a) H-plane

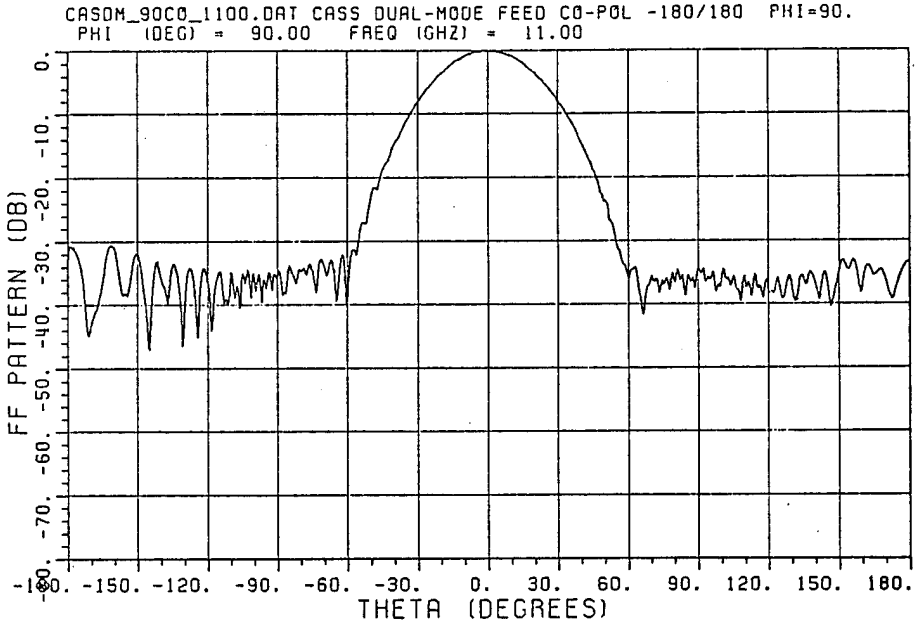

(b) E-plane

Figure 3.18. Measured patterns of the dual-mode horn for Cassegrain reflector at 11.0 GHz.

IV. SUMMARY

The method of moments is used in this report to calculate the radiation patterns of horn antennas which can be treated as bodies of revolution. The simplification derived from a rotationally symmetric body is that all physical quantities are expanded in Fourier series in the azimuth coordinate and quantities of different harmonics are treated independently [1]. The harmonics related to the horn antenna problem are those with m=1, i.e., $\cos\phi$ and $\sin\phi$.

Several examples are shown and compared with the measured patterns. Very good agreement has been obtained between calculations and measurements. One of the advantages of using the moment method instead of the well-known aperture integration method for the horn antenna problem is that the backlobes of the radiation patterns can be calculated. Also the aperture integration is not accurate for very small aperture antennas with aperture diameters less than 1.2λ.

APPENDIX A

DERIVATION OF ELEMENT OF IMPEDANCE MATRIX

A. Derivation of Equation (10)

From Equation (9) the impedance elements have the general form:

$$Z_{ln} = - \int \vec{J}_n \cdot \vec{E}^l \, ds \qquad (A.1)$$

where $\vec{J}_n$ is the expansion mode of the surface current $\vec{J}_s$ and $\vec{E}^l$ is the radiated electric field generated by the electric current mode $\vec{J}_l$. $\vec{E}^l$ can be calculated by the vector potential $\vec{A}^l$ as

$$\vec{E}^l = -j\omega \vec{A}^l + \frac{\nabla\nabla\cdot\vec{A}^l}{j\omega\mu\varepsilon}$$

$$= -j\omega \left(\vec{A}^l + \frac{\nabla\nabla\cdot\vec{A}^l}{k^2}\right) .$$

Thus, Equation (A.1) becomes

$$Z_{ln} = j\omega \int \vec{J}_n \cdot \left[\vec{A}^l + \frac{1}{k^2} \nabla\nabla\cdot\vec{A}^l\right] ds$$

$$= j\omega \int \left[\vec{J}_n \cdot \vec{A}^l + \frac{1}{k^2} \vec{J}_n \cdot (\nabla\nabla\cdot\vec{A}^l)\right] ds \qquad (A.2)$$

By using the vector identity $\nabla\cdot(f\vec{G}) = \vec{G}\cdot\nabla f + f\nabla\cdot\vec{G}$, one can express $\vec{J}_n\cdot(\nabla\nabla\cdot\vec{A}^1)$ as

$$\vec{J}_n\cdot(\nabla\nabla\cdot\vec{A}^1) = \nabla\cdot(\vec{J}_n\nabla\cdot\vec{A}^1) - (\nabla\cdot\vec{A}^1)(\nabla\cdot\vec{J}_n) .$$

Thus, Equation (A.2) becomes

$$Z_{1n} = j\omega\int \vec{J}_n\cdot\vec{A}^1\, ds + \frac{j\omega}{k^2}\int \nabla\cdot(\vec{J}_n\nabla\cdot\vec{A}^1)ds - \frac{j\omega}{k^2}\int (\nabla\cdot\vec{J}_n)(\nabla\cdot\vec{A}^1)dS. \tag{A.3}$$

From the surface form of the Divergence Theorem, the second term in (A.3) reduces to the following contour integral:

$$\frac{j\omega}{k^2}\int \nabla\cdot\left(\vec{J}_n\,\nabla\cdot\vec{A}^1\right)dS = \frac{j\omega}{k^2}\oint_c (\vec{J}_n\nabla\cdot\vec{A}^1)\cdot\hat{n}\, dl \tag{A.4}$$

where $\hat{n}$ is the outward normal of the integration contour C as shown in Figure A.1.

Because of the symmetry of the geometry, $\vec{J}_n$only has $\hat{t}$ and $\hat{\phi}$ components. For the $\hat{\phi}$ component,

$$\vec{J}_n\cdot\hat{n} = 0.$$

For the $\hat{t}$ component,

$\vec{J}_n = 0$ at the open aperture since $\vec{J}_n$ is a piecewise sinusoidal function. Consequently,

$$\frac{j\omega}{k^2} \int \nabla\cdot(\vec{J}_n \nabla\cdot\vec{A}^1)ds = 0 \quad . \tag{A.5}$$

Thus, from Equation (A.3),

$$Z_{1n} = j\omega \int \vec{J}_n \cdot \vec{A}^1 \, ds - \frac{j\omega}{k^2} \int (\nabla\cdot\vec{J}_n)(\nabla\cdot\vec{A}^1)ds \quad . \tag{A.6}$$

The vector potential $\vec{A}^1$ is given by

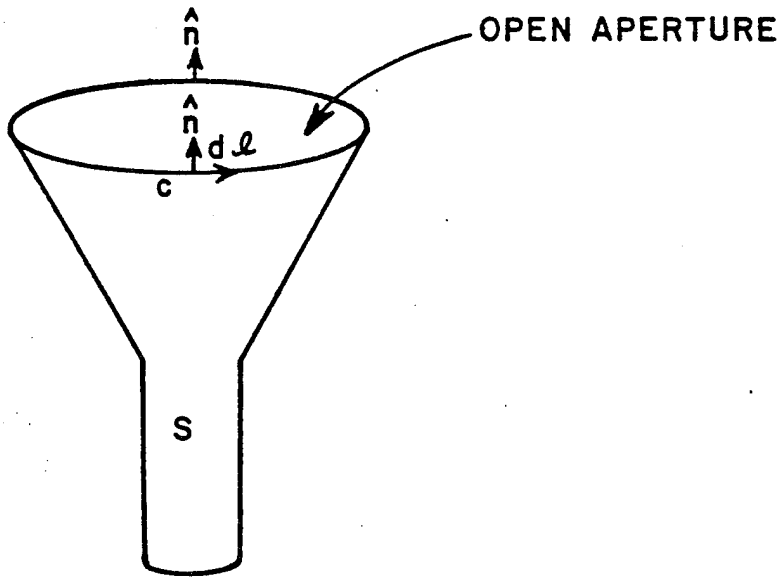

Figure A.1. Geometry for the surface form of the Divergence Theorem.

$$\vec{A}^{1} = \frac{\mu_o}{4\pi} \int \vec{J}_1 \frac{e^{-jkR}}{R} ds' \tag{A.7}$$

where R is the distance from the current $\vec{J}_1$ to $\vec{J}_n$ and the integration is carried over the location of $\vec{J}_1$. Substituting (A.7) into (A.6),

$$Z_{1n} = j\omega \frac{\mu_o}{4\pi} \iint \vec{J}_n \cdot \vec{J}_1 \frac{e^{-jkR}}{R} ds'ds - \frac{j\omega\mu_o}{4\pi k^2} \int (\nabla \cdot \vec{J}_n) \nabla \cdot \left(\int \vec{J}_1 \frac{e^{-jkR}}{R} ds' \right) ds$$

$$= \frac{j\omega\mu_o}{4\pi} \left\{ \iint \vec{J}_n \cdot \vec{J}_1 \frac{e^{-jkR}}{R} ds'ds - \frac{1}{k^2} \int \nabla \cdot \vec{J}_n \int \nabla \cdot \left(\vec{J}_1 \frac{e^{-jkR}}{R} \right) ds'ds \right\}. \tag{A.8}$$

Consider

$$\int \nabla \cdot \left(\vec{J}_1 \frac{e^{-jkR}}{R} \right) ds' = \int \left(\vec{J}_1 \cdot \nabla \left(\frac{e^{-jkR}}{R} \right) + \frac{e^{-jkR}}{R} \nabla \cdot \vec{J}_1 \right) ds'$$

$$= \int \vec{J}_1 \cdot \nabla \left(\frac{e^{-jkR}}{R} \right) ds' \tag{A.9}$$

in which $\nabla \cdot \vec{J}_1 = 0$ since $\vec{J}_1$ is the current on S′ while ∇ is operating on S. From

$$\nabla \left(\frac{e^{-jkR}}{R} \right) = - \nabla' \left(\frac{e^{-jkR}}{R} \right),$$

Equation (A.9) becomes,

$$\int \nabla\cdot\left(\vec{J}_1 \frac{e^{-jkR}}{R}\right)ds' = -\int \vec{J}_1\cdot\nabla'\left(\frac{e^{-jkR}}{R}\right)ds'$$

$$= -\int\left[\nabla'\cdot\left(\vec{J}_1\frac{e^{-jkR}}{R}\right) - \frac{e^{-jkR}}{R}\ \nabla'\cdot J_1\right]ds' \qquad (A.10)$$

The first term of Equation (A.10) can be shown as zero by changing the surface integral into a contour integral and using the same argument as the ones which lead to (A.5). Thus,

$$\int \nabla\cdot\left(\vec{J}_1\frac{e^{-jkR}}{R}\right)ds' = \int (\nabla'\cdot\vec{J}_1)\ \frac{e^{-jkR}}{R}\ ds' \qquad (A.11)$$

and Z_{ln} becomes

$$Z_{ln} = \frac{j\omega\mu_o}{4\pi}\left\{\iint \vec{J}_n\cdot\vec{J}_1\frac{e^{-jkR}}{R}\ ds'ds - \frac{1}{k^2}\int \nabla\cdot\vec{J}_n\int(\nabla'\cdot\vec{J}_1)\ \frac{e^{-jkR}}{R}\ ds'ds\right\}.$$

$$= \frac{j\omega\mu_o}{4\pi}\iint\left[\vec{J}_n\cdot\vec{J}_1 - \frac{1}{k^2}\ (\nabla\cdot\vec{J}_n)(\nabla'\cdot\vec{J}_1)\ \frac{e^{-jkR}}{R}\ ds'ds\right. \qquad (A.12)$$

as written in Equation (10).

B. Derivation of Impedance Elements $Z_{ln}^{tt}, Z_{ln}^{t\phi}, Z_{ln}^{\phi t}, Z_{ln}^{\phi\phi}$

From Equation (9),

$$Z_{ln}^{tt} = - \int \hat{t}\, J_n^t \cdot \bar{E}^{tl}\, ds$$

$$Z_{ln}^{t\phi} = - \int \hat{\phi}\, J_n^{\phi} \cdot \bar{E}^{tl}\, ds$$

$$Z_{ln}^{\phi t} = - \int \hat{t}\, J_n^t \cdot \bar{E}^{\phi l}\, ds$$

$$Z_{ln}^{\phi\phi} = - \int \hat{\phi}\, J_n^{\phi} \cdot \bar{E}^{\phi\phi}\, ds \qquad \text{(A.13)}$$

in which,

$$J_n^t = \cos m\phi \, \frac{Q_n(t)}{k\rho(t)}$$

$$J_n^{\phi} = \sin m\phi \, P_n(t)$$

and $Q_n(t), P_n(t)$ are defined in Equations (6) and (7). By using Equation (A.12),

$$Z_{ln}^{tt} = \frac{j\omega\mu_o}{4\pi} \iint \left[\hat{t}\, J_n^t \cdot \hat{t}' J_l^t - \frac{1}{k^2} (\nabla \cdot \hat{t} J_n^t)(\nabla' \cdot \hat{t}' J_l^t)\right] \frac{e^{-jkR}}{R}\, ds'ds$$

$$Z_{ln}^{t\phi} = \frac{j\omega\mu_o}{4\pi} \iint \left[\hat{\phi}\, J_n^t \cdot \hat{t}' J_l^t - \frac{1}{k^2} (\nabla \cdot \hat{\phi} J_n^\phi)(\nabla' \cdot \hat{t}' J_l^t)\right] \frac{e^{-jkR}}{R}\, ds'ds$$

$$Z_{ln}^{\phi t} = \frac{j\omega\mu_o}{4\pi} \iint \left[\hat{t}\, J_n^t \cdot \hat{\phi}' J_l^\phi - \frac{1}{k^2} (\nabla \cdot \hat{t} J_n^t)(\nabla' \cdot \hat{\phi}' J_l^\phi)\right] \frac{e^{-jkR}}{R}\, ds'ds$$

$$Z_{ln}^{\phi\phi} = \frac{j\omega\mu_o}{4\pi} \iint \left[\hat{\phi}\, J_n^\phi \cdot \hat{\phi}' J_l^\phi - \frac{1}{k^2} (\nabla \cdot \hat{\phi} J_n^\phi)(\nabla' \cdot \hat{\phi}' J_l^\phi)\right] \frac{e^{-jkR}}{R}\, ds'ds \qquad (A.14)$$

Note that $\nabla \cdot \vec{J} = \frac{1}{\rho} \frac{\partial}{\partial t} (\rho J^t) + \frac{1}{\rho} \frac{\partial}{\partial \phi} (J^\phi)$. Thus,

$$\nabla \cdot \hat{t} J_l^t = \frac{1}{\rho(t)} \frac{\partial}{\partial t} \left(\rho(t) J_l^t\right) = \frac{1}{\rho(t)} \frac{\partial}{\partial t} \left(\frac{1}{k} \cos m\phi\, Q_l(t)\right)$$

$$= \frac{1}{k\rho(t)} \cos m\phi\, Q_n'(t) \qquad (A.15)$$

$$\nabla \cdot \hat{\phi} J_l^\phi = \frac{1}{\rho(t)} \frac{\partial}{\partial \phi} (J^\phi) = \frac{1}{\rho(t)} \frac{\partial}{\partial \phi} \left(\sin m\phi\, P_l(t)\right)$$

$$= \frac{m}{\phi(t)} \cos m\phi\, P_l(t) \qquad (A.16)$$

Also,

$$\hat{t} = \hat{x}(\hat{t} \cdot \hat{\rho})(\hat{\rho} \cdot \hat{x}) + \hat{y}(\hat{t} \cdot \hat{\rho})(\hat{\rho} \cdot \hat{y}) + \hat{z}(\hat{t} \cdot \hat{z})$$

$$= \hat{x} \sin\xi \cos\phi + \hat{y} \sin\xi \sin\phi + \hat{z} \cos\xi$$

where ξ is the angle between $\hat{t}$ and $\hat{z}$.

$$\hat{\phi} = -\hat{x}\,\sin\phi + \hat{y}\,\cos\phi.$$

Similarly,

$$\hat{t}' = \hat{x}\,\sin\xi'\,\cos\phi' + \hat{y}\,\sin\xi'\,\sin\phi' + \hat{z}\,\cos\xi'$$

$$\hat{\phi} = -\hat{x}\,\sin\phi' + \hat{y}\,\cos\phi'.$$

Consequently,

$$\hat{t}\cdot\hat{t}' = \sin\xi\,\sin\xi'\,\cos(\phi-\phi') + \cos\xi\,\cos\xi'$$

$$\hat{t}\cdot\hat{\phi}' = \sin\xi\,\sin(\phi-\phi')$$

$$\hat{\phi}\cdot\hat{t}' = -\sin\xi'\,\sin(\phi-\phi')$$

$$\hat{\phi}\cdot\hat{\phi}' = \cos(\phi-\phi') \quad . \tag{A.17}$$

The distance R between $\vec{J}_1$ and $\vec{J}_n$ is given by

$$R = \left[(x-x')^2 + (y-y')^2 + (z-z')^2\right]^{1/2}$$

$$= \left[(\rho\cos\phi - \rho'\cos\phi')^2 + (\rho\sin\phi - \rho'\sin\phi')^2 + (z-z')^2\right]^{1/2}$$

$$= \left[\rho^2\cos^2\phi + \rho'^2\cos^2\phi' - 2\rho\rho' \cos\phi \cos\phi'\right.$$

$$\left. + \rho^2 \sin^2\phi + \rho'^2\sin^2\phi' - 2\rho\rho' \sin\phi \sin\phi' + (z-z')^2\right]^{1/2}$$

$$= \left[\rho^2+\rho'^2 - 2\rho\rho' \cos(\phi-\phi') + (z-z')^2\right]^{1/2}$$

$$= \left[(\rho^2 - 2\rho\rho' +\rho'^2) + (z-z')^2 + 2\rho\rho'(1-\cos(\phi-\phi'))\right]^{1/2}$$

$$= \left[(\rho-\rho')^2 + (z-z')^2 + 4\rho\rho' \sin^2 \left(\frac{\phi-\phi'}{2}\right)\right]^{1/2} \qquad \text{(A.18)}$$

where

$$\rho = \rho(t), \ \rho' = \rho'(t')$$

(1) Z_{ln}^{tt}:

$$Z_{ln}^{tt} = \frac{j\omega\mu_o}{4\pi} \iint \left[\hat{t}\, J_n^t \cdot \hat{t}' J_l^t - \frac{1}{k^2} \left(\nabla \cdot \hat{t}\, J_n^t\right)\left(\nabla' \cdot \hat{t}'\, J_l^t\right) \right] \frac{e^{-jkR}}{R}\, ds'ds$$

$$= \frac{j\omega\mu_o}{4\pi} \iint \left[\left(\hat{t} \cdot \hat{t}'\right) \cos m\phi\, \frac{Q_n(t)}{k\rho(t)} \cos m\phi'\, \frac{Q_l(t')}{k\rho'(t')} \right.$$

$$\left. - \frac{1}{k^2} \left(\frac{1}{k\rho(t)} \cos m\phi\, Q_n'(t)\right)\left(\frac{1}{k\rho'(t)} \cos m\phi'\, Q_l'(t')\right) \right] \frac{e^{-jkR}}{R}\, ds'ds$$

but $ds' = \rho'(t')\, d\phi'\, dt'$

$ds = \rho(t)\, d\phi\, dt,$

thus,

$$Z_{ln}^{tt} = \frac{j\omega\mu_o}{4\pi} \int_t \int_{t'} \int_\phi \int_{\phi'} \left[\left(\sin\xi \sin\xi' \cos(\phi-\phi') + \cos\xi \cos\xi'\right) \cos m\phi \cos m\phi' \right.$$

$$\left. \frac{Q_n(t)Q_l(t'))}{k^2} - \frac{1}{k^4} \cos m\phi \cos m\phi'\, Q_n'(t)Q_l'(t') \right] \frac{e^{-jkR}}{R}\, d\phi' d\phi\, dt' dt \qquad (A.19)$$

For the horn radiation problem, $m \neq 0$. Consider

$$\int_{\phi}\int_{\phi'} \cos(\phi-\phi') \cos m\phi \cos m\phi' \frac{e^{-jkR}}{R} d\phi' d\phi$$

$$= \frac{1}{2} \int_{\phi'}\int_{\phi} \cos(\phi-\phi')[\cos m(\phi-\phi') + \cos m(\phi+\phi')] \frac{e^{-jkR}}{R} d\phi d\phi' \tag{A.20}$$

Let $\psi=\phi-\phi'$ and noting that R is a function only of ψ, Equation (A.20) becomes

$$\frac{1}{2} \int_{\phi'=0}^{2\pi} \int_{\psi=-\phi'}^{2\pi-\phi'} \cos\psi[\cos m\psi + \cos m(\psi+2\phi')] \frac{e^{-jkR}}{R} d\psi d\phi'$$

$$= \frac{1}{2} \int_{\psi=0}^{2\pi} \int_{\phi'=0}^{2\pi} [\cos\psi\cos m\psi + \cos\psi\cos m(\psi+2\phi')] \frac{e^{-jkR}}{R} d\phi' d\psi$$

$$= \frac{1}{2} \int_{\psi=0}^{2\pi} \left\{ \cos\psi\cos m\psi \frac{e^{-jkR}}{R} \int_{\phi'=0}^{2\pi} d\phi' + \cos\psi \frac{e^{-jkR}}{R} \int_{\phi'=0}^{2\pi} \cos m(\psi+2\phi') d\phi' \right\} d\psi$$

$$= \frac{1}{2} \int_{\psi=0}^{2\pi} 2\pi \cos\psi\cos m\psi \frac{e^{-jkR}}{R} d\psi$$

$$= \pi \int_{\psi=0}^{2\pi} \cos\psi\cos m\psi \, \frac{e^{-jkR}}{R} \, d\psi$$

$$= 2\pi \int_{\psi=0}^{\pi} \cos\psi\cos m\psi \, \frac{e^{-jkR}}{R} \, d\psi$$

$$= \pi \int_{\psi=0}^{\pi} \left[\cos(m+1)\psi + \cos(m-1)\psi\right] \frac{e^{-jkR}}{R} \, d\psi \quad .$$

Let G_m be

$$G_m = \int_0^{\pi} \cos m\phi \, \frac{e^{-jkR}}{R} \, d\phi$$

thus,

$$\int_{\phi}\int_{\phi'} \cos(\phi-\phi') \, \cos m\phi \, \cos m\phi' \, \frac{e^{-jkR}}{R} \, d\phi' d\phi = \pi\left(G_{m+1} + G_{m-1}\right) \quad \text{(A.21)}$$

Consider

$$\int_{\phi}\int_{\phi'} \cos m\phi \, \cos m\phi' \frac{e^{-jkR}}{R} d\phi' d\phi = \frac{1}{2}\int_{\phi'}\int_{\phi} \left[\cos m(\phi-\phi')+\cos m(\phi+\phi')\right]\frac{e^{-jkR}}{R} \, d\phi d\phi' \quad \text{(A.22)}$$

By letting $\psi=\phi-\phi'$, (A.22) becomes

$$\frac{1}{2}\int_{\phi'=0}^{2\pi}\int_{\psi=-\phi'}^{2\pi-\phi'}\left[\cos m\psi + \cos m(\psi+2\phi')\right]\frac{e^{-jkR}}{R}\,d\psi d\phi'$$

$$= \pi\int_{0}^{2\pi}\cos m\psi\,\frac{e^{-jkR}}{R}\,d\psi$$

$$= 2\,\pi\,G_m \qquad (A.23)$$

Substituting Equations (A.21) and (A.23) into (A.19) gives

$$Z_{ln}^{tt} = \frac{j\omega\mu_o}{4\pi}\int_t\int_{t'}\left\{\pi\left(\sin\xi\sin\xi'(G_{m+1}+G_{m-1}) + 2\cos\xi\cos\xi'\right)\frac{1}{k^2}\,Q_n(t)Q_l(t')\right.$$

$$\left. - \frac{2\pi}{k^4}\,G_m Q_n'(t)Q_l'(t')\right\}dt'dt$$

$$= \frac{j\omega\mu_o}{4k^2}\int_t\int_{t'}\left\{\left(\sin\xi\sin\xi'(G_{m+1}+G_{m-1}) + 2\cos\xi\cos\xi'\right)Q_n(t)Q_l(t')\right.$$

$$\left. - \frac{2}{k^2}\,G_m Q_n'(t)Q_l'(t')\right\}dt'dt \qquad (A.24)$$

(2) $Z_{ln}^{t\phi}$:

$$Z_{ln}^{t\phi} = \frac{j\omega\mu_o}{4\pi} \iint \left[\hat{\phi}\, J_n^{\phi} \cdot \hat{t}' J_l^t - \frac{1}{k^2} \left(\nabla \cdot \hat{\phi}\, J_n^{\phi}\right)\left(\nabla' \cdot \hat{t}'\, J_l^t\right)\right] \frac{e^{-jkR}}{R}\, ds'ds$$

$$= \frac{j\omega\mu_o}{4\pi} \iint \left[\left(\hat{\phi} \cdot \hat{t}'\right) \sin m\phi\, P_n(t) \cos m\phi' \frac{Q_l(t')}{k\rho'(t')}\right.$$

$$\left. - \frac{1}{k^2} \left(\frac{m}{\rho(t)} \cos m\phi\, P_n(t)\right)\left(\frac{1}{k\rho'(t')} \cos m\phi'\, Q_l'(t')\right)\right] \frac{e^{-jkR}}{R}\, ds'ds$$

$$= \frac{j\omega\mu_o}{4\pi} \int_t \int_{t'} \int_{\phi} \int_{\phi'} \left[-\sin\xi' \sin(\phi-\phi') \sin m\phi \cos m\phi'\, P_n(t) \frac{Q_l(t')}{k\rho'(t')}\right.$$

$$\left. - \frac{1}{k^2} \frac{1}{k} \frac{m}{\rho(t)\rho'(t')} \cos m\phi \cos m\phi'\, P_n(t) Q_l'(t')\right] \cdot$$

$$\frac{e^{-jkR}}{R}\, \rho(t)\rho'(t')\, d\phi'\, d\phi\, dt'\, dt \qquad \text{(A.25)}$$

Consider ($m \neq 0$)

$$\int_{\phi} \int_{\phi'} \sin(\phi-\phi') \sin m\phi \cos m\phi' \frac{e^{-jkR}}{R}\, d\phi'\, d\phi$$

$$= \frac{1}{2} \int_{\phi'} \int_{\phi} \sin(\phi-\phi') \left[\sin m(\phi+\phi') + \sin m(\phi-\phi')\right] \frac{e^{-jkR}}{R}\, d\phi\, d\phi'$$

Since $\psi=\phi-\phi'$, the above equation becomes

$$\int_{\phi}\int_{\phi'} \sin(\phi-\phi')\sin m\phi \cos m\phi' \frac{e^{-jkR}}{R} d\phi' d\phi$$

$$= \frac{1}{2} \int_{\phi'=0}^{2\pi} \int_{\psi=-\phi'}^{2\pi-\phi'} \sin\psi \left[\sin m(\psi+2\phi') + \sin m\psi\right] \frac{e^{-jkR}}{R} d\psi d\phi'$$

$$= \frac{1}{2} \times 2\pi \int_{\psi=0}^{2\pi} \sin\psi \sin m\psi \frac{e^{-jkR}}{R} d\psi$$

$$= \frac{1}{2} \pi \int_{\psi=0}^{2\pi} [-\cos(m+1)\psi + \cos(m-1)\psi] \frac{e^{-jkR}}{R} d\psi d\phi'$$

$$= -\pi \int_{0}^{\pi} [\cos(m+1)\psi - \cos(m-1)\psi] \frac{e^{-jkR}}{R} d\psi = -\pi \left[G_{m+1} - G_{m-1}\right]$$

(A.26)

Substituting (A.26) and (A.23) into (A.25) gives

$$Z_{ln}^{t\phi} = \frac{j\omega\mu_o}{4\pi} \int_t\int_{t'} \left[\pi \frac{\rho(t)}{k} \sin\xi' \left(G_{m+1}-G_{m-1}\right)P_n(t)Q_l(t')\right.$$

$$\left. - \frac{1}{k^2} \frac{2m}{k} G_m P_n(t)Q_l'(t')\right]dt'dt$$

$$= \frac{j\omega\mu_o}{4k^2} \int_t\int_{t'} \left[k\rho(t)\sin\xi' \left(G_{m+1}-G_{m-1}\right)P_n(t)Q_l(t')\right.$$

$$\left. - \frac{2m}{k} G_m P_n(t)Q_l'(t')\right]dt'dt \qquad (A.27)$$

(3) $Z_{ln}^{\phi t}$:

$$Z_{ln}^{\phi t} = \frac{j\omega\mu_o}{4\pi} \iint \left[\hat{t}\, J_n^t \cdot \hat{\phi}'\, J_l^\phi - \frac{1}{k^2} (\nabla\cdot\hat{t}\, J_n^t)(\nabla'\cdot\hat{\phi}'\, J_l^\phi)\right] \frac{e^{-jkR}}{R} ds'ds$$

$$= \frac{j\omega\mu_o}{4\pi} \int_t\int_{t'}\int_\phi\int_{\phi'} \left[\sin\xi\sin(\phi-\phi')\cos m\phi \frac{Q_n(t)}{k\rho(t)} \sin m\phi' P_l(t')\right.$$

$$\left. - \frac{1}{k^2} \left(\frac{1}{k\rho(t)} \cos m\phi\, Q_n'(t)\right)\right.$$

$$\left. \cdot \left(\frac{m}{\rho'(t')} \cos m\phi' P_l(t')\right) \frac{e^{-jkR}}{R} \rho(t)\rho'(t')\, d\phi'd\phi\, dt'dt\right]$$

(A.28)

It can be shown that

$$\int_{\phi}\int_{\phi'} \sin(\phi-\phi')\cos m\phi \sin m\phi' \frac{e^{-jkR}}{R} d\phi' d\phi = \pi\left(G_{m+1}-G_{m-1}\right) \quad (A.29)$$

Substituting (A.29), (A.23) into (A.28) gives

$$Z_{ln}^{\phi t} = \frac{j\omega\mu_o}{4\pi}\int_t\int_{t'}\left[\pi\frac{1}{k\rho(t)}\sin\xi\left(G_{m+1}-G_{m-1}\right)Q_n(t)P_1(t')\right.$$

$$\left. - \frac{\pi}{k^2}\frac{2m}{k\rho(t)\rho'(t')}G_m Q_n'(t)P_1(t')\right]\rho(t)\rho'(t')\,dt'dt$$

$$= \frac{j\omega\mu_o}{4k^2}\int_t\int_{t'}\left[k\rho'(t')\sin\xi\left(G_{m+1}-G_{m-1}\right)Q_n(t)P_1(t')\right.$$

$$\left. - \frac{2m}{k}G_m Q_n'(t)P_1(t')\right]dt'dt \quad (A.30)$$

(4) $Z_{ln}^{\phi\phi}$:

$$Z_{ln}^{\phi\phi} = \frac{j\omega\mu_o}{4\pi}\iint\left[\hat{\phi}\,J_n^{\phi}\cdot\hat{\phi}'\,J_1^{\phi} - \frac{1}{k^2}\left(\nabla\cdot\hat{\phi}\,J_n^{\phi}\right)\left(\nabla'\cdot\hat{\phi}'\,J_1^{\phi}\right)\right]\frac{e^{-jkR}}{R}\,ds'ds$$

$$= \frac{j\omega\mu_o}{4\pi}\int_t\int_{t'}\int_{\phi}\int_{\phi'}\left[\cos(\phi-\phi')\sin m\phi\,P_n(t)\sin m\phi'\,P_1(t')\right.$$

$$\left. - \frac{1}{k^2}\left(\frac{m}{\rho(t)}\cos m\phi\,P_n(t)\right)\left(\frac{m}{\rho'(t')}\cos m\phi'\,P_1(t')\right)\right]$$

$$\cdot\frac{e^{-jkR}}{R}\rho(t)\rho'(t')\,d\phi'd\phi\,dt'dt \quad (A.31)$$

Again, it can be shown that

$$\int_{\phi}\int_{\phi'} \cos(\phi-\phi') \sin m\phi \sin m\phi' \frac{e^{-jkR}}{R} d\phi' d\phi = \pi\left(G_{m+1}+G_{m-1}\right) \quad (A.32)$$

Substituting (A.32), (A.23) into (A.31) gives

$$Z_{ln}^{\phi\phi} = \frac{j\omega\mu_o}{4\pi} \int_t\int_{t'} \left[\pi\rho(t)\rho'(t')\left(G_{m+1}+G_{m-1}\right)P_n(t)P_l(t')\right.$$

$$\left. - \frac{2m^2}{k^2} \pi G_m P_n(t)P_l(t')\right] \frac{e^{-jkR}}{R} dt'dt$$

$$= \frac{j\omega\mu_o}{4k^2} \int_t\int_{t'} \left[k^2\rho(t)\rho'(t')\left(G_{m+1}+G_{m-1}\right)-2m^2G_m\right]P_n(t)P_l(t') \, dt'dt$$

(A.33)

REFERENCES

[1] J.R. Mautz and R.F. Harrington, "Radiation and Scattering from Bodies of Revolution," Appl. Sci. Res. 20, pp. 405-435, June 1969.

[2] A.J. Terzuoli, Jr., C.W. Chuang and L. Peters, Jr., "An Integral Equation Approach to Obtain the Significant Parameters of Dihedral Corrugated Horns," Report 3821-2, The Ohio State University ElectroScience Laboratory, Department of Electrical Engineering, July 1976.

[3] J.H. Richmond, "Radiation and Scattering by Thin-Wire Structures in the Complex Frequency Domain," Technical Report 2902-10, The Ohio State University ElectroScience Laboratory, Department of Electrical Engineering, July 1973.